Journal of Medicinal Chemistry

Article

pubs.acs.org/jmc

Symmetric Bis-chalcones as a New Type of Breast Cancer Resistance Protein Inhibitors with a Mechanism Different from That of Chromones

Evelyn Winter,[†,‡] Patrícia Devantier Neuenfeldt,[§] Louise Domeneghini Chiaradia-Delatorre,[§] Charlotte Gauthier,[†] Rosendo Augusto Yunes,[§] Ricardo José Nunes,[§] Tânia Beatriz Creczynski-Pasa,[‡] and Attilio Di Pietro*[,†]

[†]Equipe Labellisée Ligue 2014, BMSSI UMR5086 CNRS/Université Lyon 1, IBCP, 69367 Lyon, France

[‡]Department of Pharmaceutical Sciences, PGFAR, Federal University of Santa Catarina, 88040-900 Florianopolis, Santa Catarina, Brazil

[§]Department of Chemistry, Federal University of Santa Catarina, 88040-900 Florianopolis, Santa Catarina, Brazil

ABSTRACT: Potent ABCG2 inhibitors were recently identified as asymmetric chromones with different types of substituents. We here synthesized symmetric bis-chalcones that were differently substituted and screened for their ability to inhibit mitoxantrone efflux from ABCG2-transfected HEK293 cells. Potent bis-chalcone inhibitors were identified, the efficiency depending on both position of the central ketone groups and the number and positions of lateral methoxy substituents. The best derivative, namely, **1p**, was selective for ABCG2 over P-glycoprotein and MRP1, appeared not to be transported by ABCG2, and was at least as active on various drug-selected cancer cells overexpressing ABCG2. Compound **1p** stimulated the ABCG2 basal ATPase activity by contrast to a chromone lead that inhibited it, suggesting different mechanisms of interaction. Combination of both types of inhibitors produced synergistic effects, leading to complete inhibition at very low concentrations.

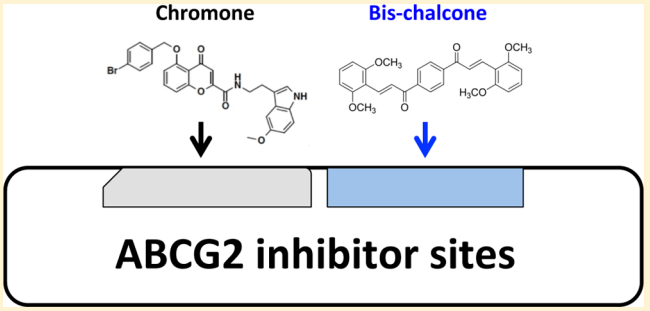

INTRODUCTION

One major obstacle for treating tumors by chemotherapy is cancer cell multidrug resistance, which may be caused by several factors including the overexpression of ATP-binding cassette (ABC) transporters. These transporters are transmembrane proteins working as efflux pumps to reduce the intracellular concentration of drugs.[1,2] A total of 48 genes encode ABC transporters in humans, of which only three are recognized to be associated with low prognostic in cancer patients: ABCB1/P-glycoprotein, ABCC1/MRP1 (multidrug resistance protein 1), and ABCG2/BCRP (breast cancer resistance protein).[3] P-glycoprotein (P-gp) was the first multidrug ABC transporter to be discovered and extensively studied.[4] MRP1 was later also associated with multidrug resistance,[5] while BCRP was more recently identified.[6−8]

One of the strategies to eliminate resistant tumors is to use inhibitors of the multidrug ABC transporters. Combination of inhibitors with anticancer drugs should increase drug accumulation inside the cell. In vitro, a number of P-gp inhibitors have been optimized up to third- or fourth-generation compounds, but their intrinsic toxicity and low in vivo activity prevented finalizing of clinical trials.[9−11]

ABCG2 is a protein composed of 655 aminoacids, constituting a "half-transporter" containing only one cytosolic nucleotide-binding domain and one transmembrane domain with six α-helical spans. This transporter is present in various membrane barriers protecting sensitive organs, as well as in many types of cancer concerning breast, lung, pancreas, colon, and leukemias.[12,13] The first specific ABCG2 inhibitor of natural origin was fumitremorgin C (FTC), which displayed a serious neurotoxicity.[14] Synthetic derivatives were developed resulting in highly potent Ko143, which still retained some residual toxicity.[15,16] New-generation inhibitors of other types have been developed, but very few have been tested with in vivo animal models.[17]

Screening of different classes of flavonoids identified interesting inhibitors such as hydrophobic flavones[18,19] and asymmetric chalcones with a variety of substituents[20−22] for establishing structure−activity relationships. The best compound recently identified to be nearly as potent as Ko143 was chromone **6g**,[23] which in this work was renamed as chromone **1** (Figure 1) for the comparative study with a number of derivatives to characterize the inhibition mechanism toward both drug efflux and ATPase activity.[24] In the present work, to better understand the structure−activity relationships and their

Received: December 6, 2013
Published: March 10, 2014

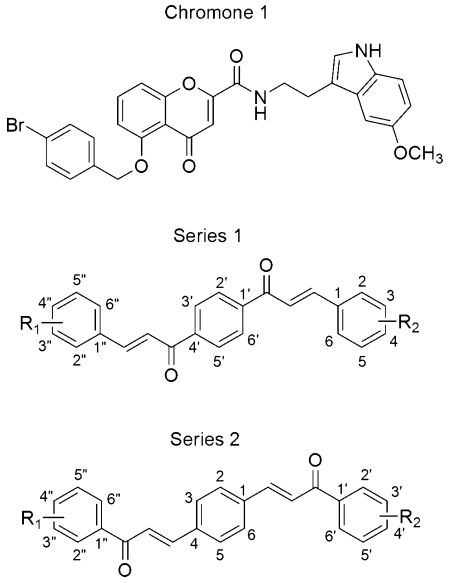

Figure 1. Structures of the previously published chromone **1**[23] and the two series of novel bis-chalcones.

influence on the interaction with ABCG2 protein, we synthesized two series of symmetric bis-chalcones (series **1** and series **2**), by varying the position of central carbonyls and the number and nature (essentially methoxy) of substituents on the lateral phenyl rings (Figure 1). The best compounds were found to be potent and selective and, interestingly, to bind to a different site than chromone **1** allowing combinations.

CHEMISTRY

The access to series **2** is shown in Table 1. Bis-chalcones **2a**–**p** were synthesized according to a previously reported method of chalcones synthesis.[25] These compounds were obtained by the reaction between terephthalaldehyde with substituted acetophenones, using 50% KOH in methanol, to provide the final compounds with yields in the range 62–92%. All reagentes were commercially available except 2,4,5-trimethoxyacetophenone (synthesized as previously described with 81% yield)[26] and 2,4,6-trimethoxyacetophenone (synthesized as previously described with 85% yield).[27]

The preparation scheme of derivatives belonging to series **1** is also shown in Table 1. The reactions conditions were the same as those used for the series **2** of bis-chalcones. The 1,4-diacetylbenzene reacts with substituted benzaldehydes in the presence of 50% KOH and methanol, providing analogues **1a**–**q** with yields in the range 59–93%.

The bis-chalcones **1a**, **1c**, **1f**, **1h**, **1k**, **1l**, **1n**, **2a**, **2d**, **2e**, **2h**, **2j**, **2k**, **2o**, and **2p** have already been reported in the literature,[28] and **1b**, **1d**, **1e**, **1g**, **1i**, **1j**, **1m**, **1o**, **1p**, **1q**, **2b**, **2c**, **2f**, **2g**, **2i**, **2l**, **2m**, and **2n** are novel compounds.

All synthesized compounds were fully characterized by melting points, ^{1}H NMR, and ^{13}C NMR and confirmed by mass spectrometry (see the Experimental Section). High resolution mass spectra are in agreement with the exact mass, confirming ≥95% purity. In ^{1}H NMR spectra of compounds, the aromatic hydrogens appear at 6.5–8.5 ppm depending on the substituent on the aromatic (Ar) group. The singlet signals at the region between 7.5 and 8.5 ppm are attributed to the resonance of the 1,4-phenylene ring hydrogens. The doublet signals with $J \approx 16$ Hz at the region between 7.0 and 8.0 ppm are due to the resonance of the double-bond hydrogens adjacent to the carbonyl group (Hα and Hβ). The ^{13}C NMR spectra of the compounds showed signals between 100.0 and 160.0 ppm due to the resonance of aryl and unsaturated carbons. The signals at the region between 180 and 190 ppm attributed to the carbon resonance of the C═O group are consistent with the expected structures.

BIOLOGICAL EVALUATION

Structure–Activity Relationships toward Inhibition of ABCG2-Mediated Drug Efflux. The 33 synthesized symmetric bis-chalcones, constituting the series **1** and **2** that differ by the central carbonyls position, were analyzed for their ability to inhibit mitoxantrone efflux and then to increase its accumulation in *ABCG2*-transfected HEK293 cells (Table 1).

The proximity of the carbonyl with the central phenyl ring in the series **1** seems to be more favorable toward inhibition when comparing **1i** (96% inhibition at 5 μM, EC_{50} = 0.3 μM) to **2m** (41% inhibition), **1k** (92% inhibition, EC_{50} = 0.4 μM) to **2o** (66% inhibition, EC_{50} = 1.8 μM), and **1e** (96% inhibition, EC_{50} = 0.7 μM) to **2g** (74% inhibition, EC_{50} = 1.3 μM). However, an opposite effect was observed in **1b** (43% inhibition) versus **2b** (73% inhibition) and in **1c** (63% inhibition, EC_{50} = 2.1 μM) versus **2d** (97% inhibition, EC_{50} = 0.8 μM), suggesting that the dependence on carbonyl position was modulated by the substituents present on the lateral A and B phenyl rings.

In both series, the inhibition efficiency was highly dependent on methoxy substituents, since all of the 14 most potent compounds, for which the EC_{50} values were determined as illustrated in Figure 2, contained one (**2c** and **2l**), two (**1c**, **1e**, **1p**, **2d**, **2e**, **2g**, and **2i**), or three (**1i**, **1k**, **1q**, **2b**, and **2o**) methoxy groups. This contrasted with the low efficiency observed in their absence (in compounds **1d**, **1f**, **1g**, **1h**, **1j**, **1m**, **1n**, **1o**, **2f**, **2h**, **2j**, **2k**, and **2n**).

The position of methoxy substituents was critical for activity, with the following preference: position 2′ (**2l**, 95% inhibition, EC_{50} = 1.1 μM) > 3′ (**2c**, 73% inhibition, EC_{50} = 2.3 μM) > 4′ (**2a**, 27% inhibition). It is notable that compounds with only one methoxy group at position 4′ (**2a** and **1a**) did not show a significant activity. In addition, the substitution of the methoxy group by a hydrophilic hydroxyl substituent at position 4′ clearly resulted in a negative effect on activity when comparing **2p** (only 28% inhibition) and **1l** (no inhibition) with **2d** (97% inhibition) and **1c** (63% inhibition). Methoxy groups at positions 6′ and 5′ were also favorable, since the inhibitor leads of each series were **1p** (2′,6′-dimethoxy, EC_{50} = 0.2 μM) and **2i** (3′,5′-dimethoxy, EC_{50} = 0.5 μM). Within the series **2**, except for **2l**, the methoxy substituents at meta positions (3′ and 5′) appeared to bring the best contribution to inhibition potency (in **2b**, **2c**, **2d**, **2g**, and **2i**), in contrast to the series **1** where the ortho positions (2′ and 6′) were better (in **1e**, **1i**, **1k**, **1p**, and **1q**). This might indicate the role of electron density of the rings or the contribution of steric effects.

Inhibition of Cancer Cells Overexpressing ABCG2, Selectivity toward ABCG2, and Chemosensitization of Cell Growth. The action mechanism of symmetric bis-chalcones was further investigated with the lead compound of each series (**1p** and **2i**). The inhibitory effects were first evaluated in mitoxantrone-selected cancer cell lines, which were demonstrated to overexpress ABCG2, namely, lung cancer H460[29] and H23[30] cell lines and pancreatic PANC-1 cell line.[31] Table 2 shows that **1p** displayed the same efficiency on H23 and PANC-1 (EC_{50} = 0.2 μM) and an even 3-fold higher

dx.doi.org/10.1021/jm401879z | J. Med. Chem. 2014, 57, 2930–2941

Table 1. Inhibition of ABCG2-Mediated Mitoxantrone Efflux by Differently Substituted Bis-chalcones

Series 1

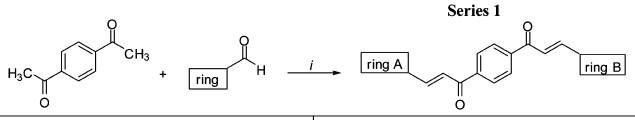

Compound	A-ring = B-ring	Inhibition at 5 μM (%)[a]	EC_{50} (μM)[b]	Compound	A-ring = B-ring	Inhibition at 5 μM (%)[a]	EC_{50} (μM)[b]
1a	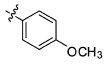	18 ± 5		**1j***	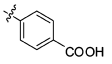	2 ± 2	
1b*	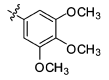	43 ± 17		**1k**	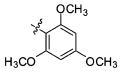	92 ± 8	0.40 ± 0.02
1c	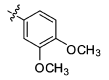	63 ± 7	2.1 ± 0.4	**1l**	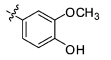	0 ± 3	
1d*		11 ± 2		**1m***	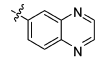	18 ± 2	
1e*	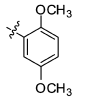	96 ± 7	0.70 ± 0.02	**1n**	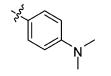	34 ± 1	
1f		7 ± 6		**1o***	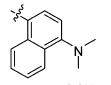	17 ± 7	
1g*		13 ± 1		**1p***	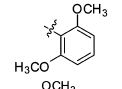	108 ± 1	0.20 ± 0.04
1h		13 ± 1		**1q***	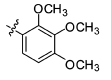	86 ± 1	1.4 ± 0.6
1i*	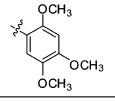	96 ± 5	0.30 ± 0.07				

Series 2

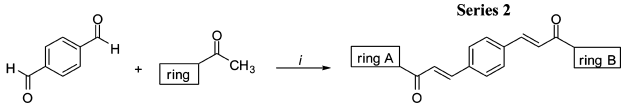

Compound	A-ring = B-ring	Inhibition at 5 μM (%)[a]	EC_{50} (μM)[b]	Compound	A-ring = B-ring	Inhibition at 5 μM (%)[a]	EC_{50} (μM)[b]
2a	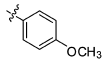	27 ± 4		**2i***	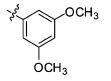	78 ± 4	0.5 ± 0.3
2b*	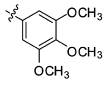	73 ± 15	1.1 ± 0.1	**2j**		23 ± 3	
2c*	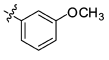	73 ± 5	2.3 ± 0.2	**2k**		25 ± 3	
2d	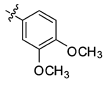	97 ± 19	0.8 ± 0.3	**2l***		95 ± 15	1.1 ± 0.1
2e	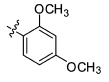	86 ± 18	0.9 ± 0.1	**2m***	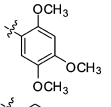	41 ± 5	
2f*		19 ± 1		**2n***	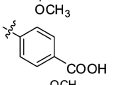	0 ± 1	
2g*		74 ± 1	1.3 ± 0.2	**2o**	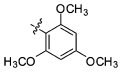	66 ± 15	1.8 ± 0.4
2h		45 ± 2		**2p**	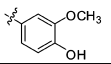	28 ± 7	

(i) Methanol, 50% KOH, rt, 16 h. The asterisk (*) indicates novel compounds. [a]Mitoxantrone efflux was determined by measuring its cellular accumulation by flow cytometry, relative to ABCG2-negative control cells. For high-affinity compounds, the maximal inhibition was observed at 5 μM. [b]EC_{50} values were calculated by GraphPad Prism5 as the bis-chalcone concentrations producing half-maximal inhibition after incubating the cells with increasing concentrations up to 10 μM. Data are the mean ± SD of at least three independent experiments.

dx.doi.org/10.1021/jm401879z | J. Med. Chem. 2014, 57, 2930−2941

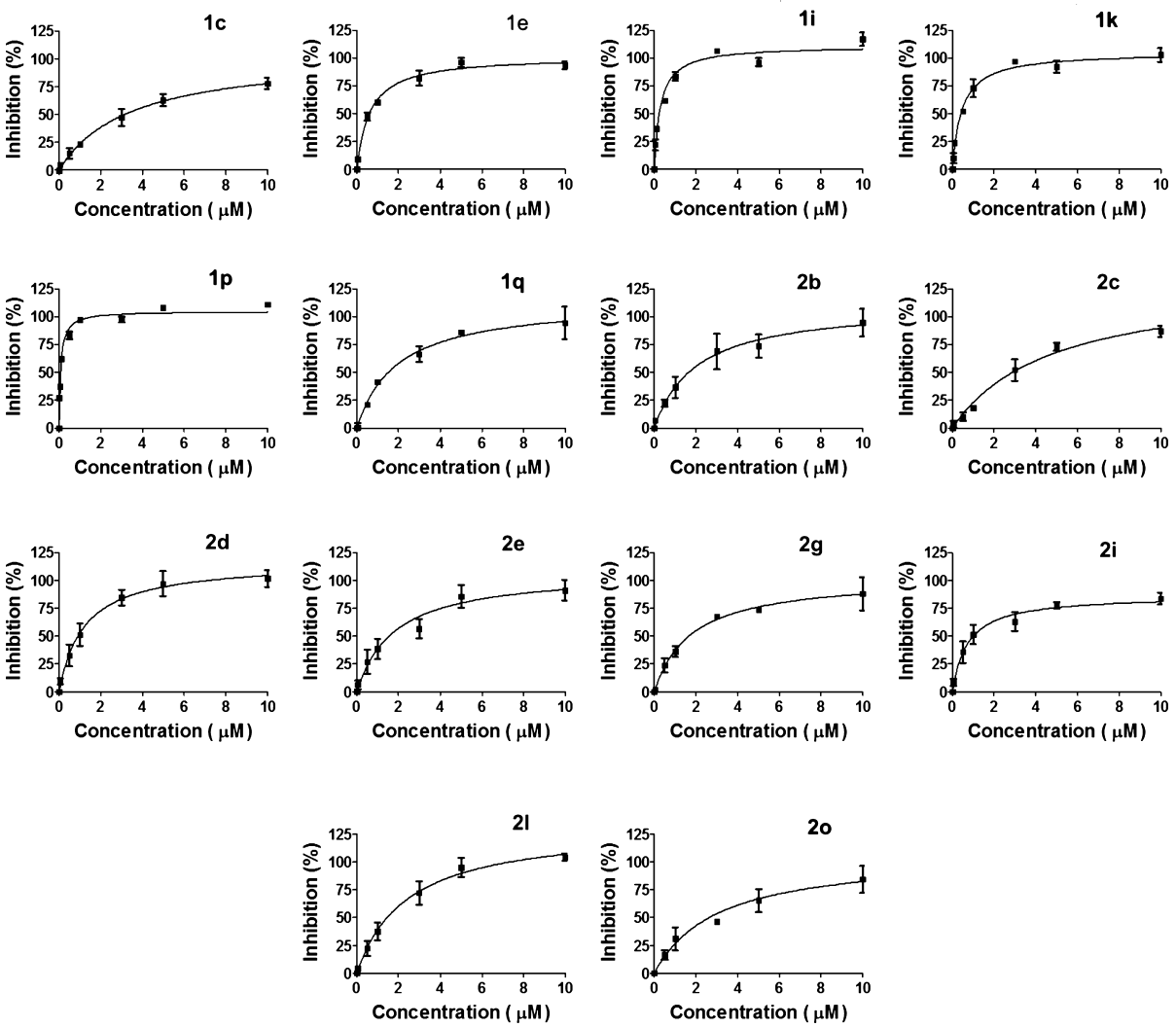

Figure 2. Concentration dependence of mitoxantrone-efflux inhibition by symmetric bis-chalcones in HEK293-tranfected cells. The curves are fitted with GraphPad Prism5 and illustrate the EC_{50} values of the best compounds identified in Table 1. Data are the mean ± SD of at least three independent experiments.

Table 2. Ability of the Bis-chalcone Leads to Inhibition of Different Cancer Cell Lines Overexpressing ABCG2[a]

	EC_{50} (μM)	
ABCG2-overexpressing cancer cells	**1p**	**2i**
mitoxantrone-selected H460	0.08 ± 0.01	1.63 ± 0.08
mitoxantrone-selected H23	0.22 ± 0.11	1.17 ± 0.71
mitoxantrone-selected PANC-1	0.21 ± 0.18	0.21 ± 0.18

[a]The EC_{50} values of inhibition, on ABCG2-mediated mitoxantrone efflux, by both bis-chalcone leads were determined on various drug-selected cancer cell lines, as described in Table 1 for transfected cells.

potency in H460 cells, with a very low EC_{50} value of 80 nM. As for *ABCG2*-transfected cells, **2i** seemed to be less potent than **1p**, but the EC_{50} values remained in the micromolar range (0.2−1.6 μM).

The two bis-chalcone leads (**1p** and **2i**) were not able, at up to 10 μM, to inhibit the drug-efflux activity of either P-glycoprotein toward mitoxantrone or MRP1 toward calcein (Figure 3). This indicated that these bis-chalcones behave as ABCG2-selective inhibitors.

The inhibition by **1p** and **2i** on ABCG2-mediated mitoxantrone efflux was confirmed by their ability to sensitize to mitoxantrone toxicity the cell growth of *ABCG2*-transfected cells, as monitored by MTT assays (Figure 4). The IC_{50} (cytotoxic concentration for 50% cell survival) of mitoxantrone in *ABCG2*-transfected cells (26.6 nM) was decreased to 7.2 or 7.6 nM, respectively, in the presence of **1p** or **2i** at low concentrations, namely, 0.1 and 0.5 μM, which were not cytotoxic. These results showed that symmetric bis-chalcones can fully chemosensitize the ABCG2-overexpressing cells, since mitoxantrone presented an IC_{50} of 10 nM in control, sensitive HEK293 cells. At increasing concentrations, the **1p** and **2i** cytotoxicity on cell growth was not lower in *ABCG2*-transfected cells than in control cells, indicating no cross-resistance, which suggested the lack of any apparent transport by ABCG2 (data not shown).

Effects on Basal and Drug-Stimulated ATPase Activity. The effects of the bis-chalcone leads **1p** and **2i**

dx.doi.org/10.1021/jm401879z | J. Med. Chem. 2014, 57, 2930−2941

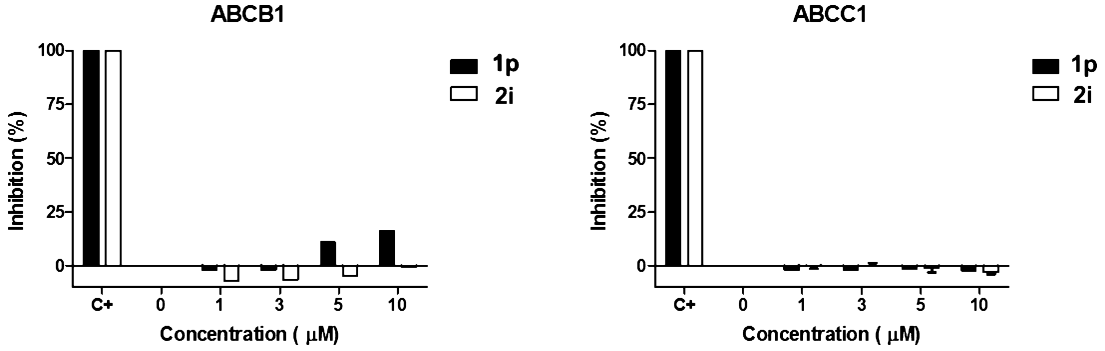

Figure 3. Effects of the bis-chalcone leads on drug efflux mediated by either P-glycoprotein or MRP1. Each bis-chalcone was assayed up to 10 μM for its ability to alter the P-glycoprotein-mediated mitoxantrone efflux in *ABCB1*-transfected NIH-3T3 (A) or the MRP1-mediated calcein efflux in *ABCC1*-transfected HEK293 cells (B), as determined by flow cytometry. The inhibition was calculated relative to control cells, not expressing the transporter, displaying by a maximal drug accumulation.

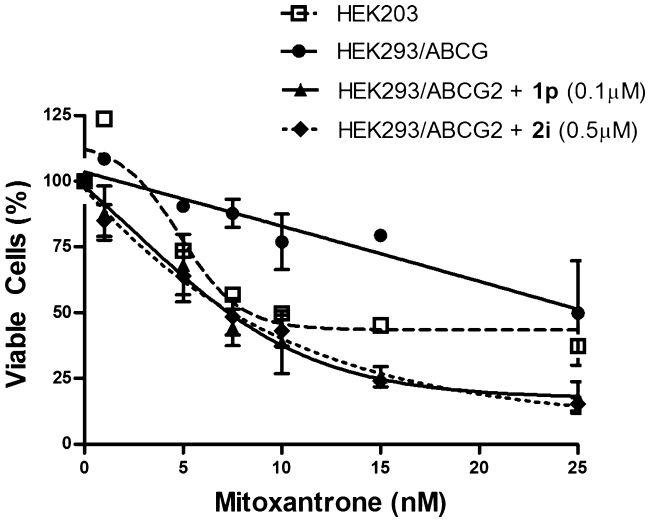

Figure 4. Sensitization of cell growth to mitoxantrone. The viability of HEK293-*ABCG2* cells was evaluated by MTT assays after a 72 h incubation with mitoxantrone (at 0–25 nM) in the absence of bis-chalcone (filled circles) or with 0.1 μM **1p** (filled triangles) or 0.5 μM **2i** (empty circles). Parallel experiments were performed without bis-chalcone and in HEK293-*pcDNA3.1* (empty squares).

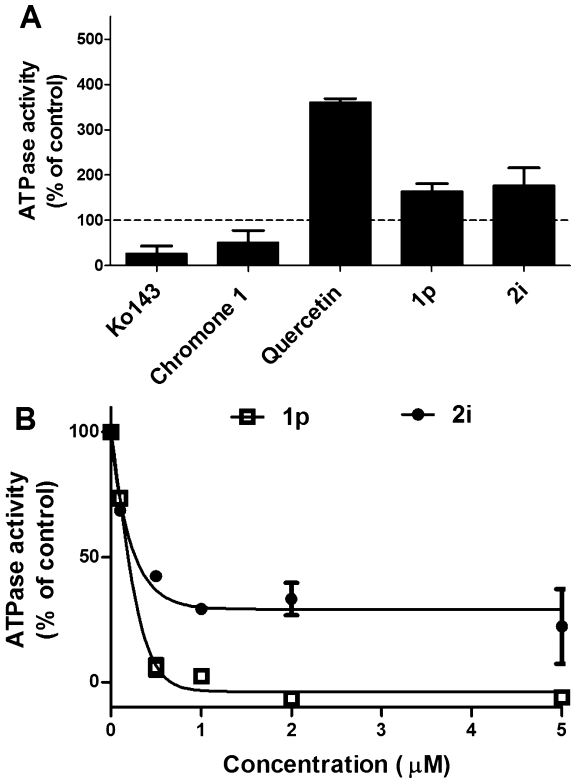

Figure 5. Effects of **1p** and **2i** on ABCG2 basal and substrate-stimulated ATPase activity. The effects of the different compounds on vanadate-sensitive ATPase activity of ABCG2 were tested using 10 μg/sample of ABCG2-containing membrane vesicles (prepared from Sf9 cells overexpressing human ABCG2 and loaded with cholesterol). The experiments were performed in the absence of transport substrate (A) or with 2 μM quercetin, where the coupled ATPase activity was the difference between total and basal activities (B). The specific basal and coupled ATPase activities, taken as 100%, were respectively 7.0 ± 0.4 and 18.3 ± 0.5 nmol of ATP hydrolyzed/min × mg of proteins.

were studied on the ATPase activity of Sf9 insect cell membranes overexpressing human ABCG2,[32] which were supplemented with cholesterol to generate a maximal vanadate-sensitive activity.[33] The "basal" ATPase activity, measured in the absence of substrate drug, was strongly inhibited by Ko143 and chromone **1** (Figure 5A). Interestingly, it was not inhibited but, on the contrary, stimulated by **1p** and **2i** 1.6-fold and 1.8-fold respectively, similar to the transported substrate quercetin, which produced a 3.6-fold stimulation.

The "coupled", or "drug-stimulated", ATPase activity observed in the presence of 2 μM quercetin was highly dependent on **1p** concentration, a complete inhibition being produced with an IC_{50} value (concentration producing 50% inhibition of activity) of around 0.19 μM (Figure 5B). For **2i**, a slightly lower-affinity inhibition was observed (IC_{50} = 0.27 μM), and the maximal inhibition was limited to 72%.

The less potent inhibition of drug efflux produced by bis-chalcones, especially **2i**, by comparison to chromone **1** and Ko143 might be related, at least partly, to their stimulation, in contrast to inhibition, of basal ATPase activity.

Combination of 1p with Inhibitors of Different Mechanism. The stimulation produced by **1p** on the basal ATPase activity suggested a distinct binding site compared with two other potent inhibitors, Ko143 and chromone **1**, that inhibit such activity. The inhibition affinity of **1p** was therefore investigated in combination with low concentrations of either chromone **1** or Ko143 (0.1 or 0.02 μM, respectively, producing around 50% inhibition). Interestingly, synergistic effects were

dx.doi.org/10.1021/jm401879z | J. Med. Chem. 2014, 57, 2930–2941

obtained in all cases: the highest effect was observed with chromone **1**, which increased by 15-fold the inhibition affinity of **1p** (Table 3), while a lower effect was induced by Ko143 (1.8-fold increase). Similarly, a low concentration of **1p** (0.1 μM) was able to increase the inhibition affinity of chromone **1** (by 3-fold) and of Ko143 (by 2.4-fold).

Table 3. Synergistic Combinations of 1p with Other Inhibitors[a]

studied inhibitor	additional inhibitor	EC_{50} (μM)	increased affinity (fold)
1p alone		0.227 ± 0.043	
	+chromone **1** (0.1 μM)	0.015 ± 0.010**	15
	+Ko143 (0.02 μM)	0.126 ± 0.025*	1.8
chromone **1** alone		0.094 ± 0.001	
	+**1p** (0.1 μM)	0.031 ± 0.015**	3.0
Ko143 alone		0.029 ± 0.008	
	+**1p** (0.1 μM)	0.012 ± 0.007	2.4

[a]The EC_{50} value of inhibition, on ABCG2-mediated mitoxantrone efflux from transfected HEK293 cells, was determined first for each inhibitor used alone and then in the presence of the indicated additional inhibitor producing around 50% inhibition. The increased affinity of inhibition was the ratio of EC_{50} values without inhibitor to EC_{50} with additional inhibitor. Data are the mean ± SD of at least three independent experiments. The *t*-test compared all combinations including additional inhibitors with the studied inhibitor alone: (*) $p < 0.05$ and (**) $p < 0.01$.

DISCUSSION

The present analysis of 33 bis-chalcones has shown for the first time the interest of symmetric, methoxy-substituted, inhibitors of ABCG2 through their inhibition potency, even on cancer cell lines, their selectivity and apparent absence of transport, and finally their different binding site and/or inhibition mechanism versus other known inhibitors allowing synergistic combinations at low concentrations.

Originality of Symmetric ABCG2 Inhibitors. Our finding that the best symmetric bis-chalcones behave as potent ABCG2 inhibitors, with submicromolar EC_{50} values, is consistent with the high-affinity inhibition produced by dimeric inhibitors on P-glycoprotein.[34,35] Of special interest were flavonoid dimers shown to be active on both P-glycoprotein[36,37] and MRP1,[38] bringing attention to their potential application to ABCG2. The positive role of methoxy substituents toward ABCG2 inhibition agrees with previous observations with methoxy *trans*-stilbenes,[39] asymmetric chalcones,[20,21] and chromones.[23] However, as shown for P-glycoprotein, other structural parameters in addition to methoxy substituents might be critical for inhibition.[40−42] Bis-chalcones behave as selective inhibitors of ABCG2 over P-glycoprotein and MRP1, as for other flavonoidic compounds, and appear not to be transported on the basis of the absence of cross-resistance, in contrast to transport substrates.

The main originality of bis-chalcones **1p** and **2i** versus other known potent inhibitors, such as Ko143 and chromone **1** which inhibit the basal ATPase activity,[24] is that they stimulate such an activity, similar to transport substrates.[24] Therefore, the bis-chalcone leads appear to mimic substrates without being transported. This indicates that symmetric bis-chalcones obey a different interaction mechanism than the asymmetric inhibitors chromone **1** and Ko143.

Synergistic Combinations of Asymmetric and Symmetric Inhibitors at Low Concentrations. The synergistic inhibitions observed for all combinations of inhibitors at low concentrations, as also observed for some P-glycoprotein inhibitors,[42] suggest that both types of inhibitors may bind to distinct sites within ABCG2, which however requires to be further proven by direct structural data. The highest synergism, observed with a low concentration of chromone **1** increasing to 15-fold the inhibition affinity toward **1p**, might be due to a proximity of the two inhibitory sites. This agrees with the recent observation that chromone **1** binding could be shifted upon a slight substituent modification leading to stimulation of basal ATPase activity.[24] Such a high synergism presents the great advantage to reach a complete inhibition of drug efflux by using very low concentrations of both inhibitors, within the nanomolar range. This should be actually useful for future in vivo assays in animal models, by limiting cytotoxicity and related side effects. This should further improve the already promising in vivo activity in mice of chromone **1** to sensitize xenografted tumor growth to chemotherapy.

EXPERIMENTAL SECTION

Chemistry. Preparation of Compounds. Reagents used were obtained commercially (Sigma-Aldrich), except 2,4,5-trimethoxyacetophenone and 2,4,6-trimethoxyacetophenone, synthesized as previously described.[26,27]

General Procedure for the Preparation of the Series 1 of Bis-chalcones. Bis-chalcones **1a−q** were prepared by aldolic condensation between 1,4-diacetylbenzene (1.0 mmol) and corresponding benzaldehydes (2.0 mmol) in methanol (25 mL) and KOH (50% w/v) at room temperature and with magnetic stirring for 24 h. Distilled water and 10% hydrochloric acid solution were added for total precipitation of the compounds, which were obtained by vacuum filtration and then recrystallized in ethanol. The purity of the synthesized bis-chalcones **1a−q** was analyzed by melting points and by thin−layer chromatography (TLC) using Merck silica precoated aluminum plates of 200 μm thickness, with several solvent systems of different polarities. Compounds were visualized with ultraviolet light (λ = 254 and 360 nm) and using sulfuric vanillin solution followed by heat application as developing agent.

General Procedure for the Preparation of the Series 2 of Bis-chalcones. Bis-chalcones **2a−p** were prepared by aldolic condensation between terephthaldeyde (1.0 mmol) and corresponding acetophenones (2.0 mmol) in methanol (25 mL) and KOH (50% w/v) at room temperature and with magnetic stirring for 24 h. Distilled water and 10% hydrochloric acid solution were added for total precipitation of the compounds, which were obtained by vacuum filtration and then recrystallized in ethanol. The purity of the synthesized bis-chalcones **2a−p** was analyzed in the same way as for the series **1**.

Physicochemical Data of the Synthesized Compounds. All compounds were characterized by melting points (mp) and ^{1}H and ^{13}C nuclear magnetic resonance spectroscopy (NMR) and confirmed by mass spectrometry. Melting points were determined with a Microquímica MGAPF-301 apparatus and are uncorrected. NMR (^{1}H and ^{13}C) spectra were recorded on a Bruker Ac-200F (200 MHz) or on a Varian Oxford AS-400 (400 MHz) instrument, using tetramethylsilane as internal standard.

High-resolution mass spectra were recorded on a micrOTOF-QII (Bruker Daltonics) mass spectrometer equipped with an automatic syringe pump (KD Scientific) for sample injection (constant flow of 3 μL/min), by positive mode of electron spray ionization (ESI-MS) technique (4.5 kV and 180 °C). An acetonitrile/methanol mixture was used as solvent. The instrument was calibrated in the range m/z 50−3000 using an internal calibration standard (low concentration tuning

dx.doi.org/10.1021/jm401879z | J. Med. Chem. 2014, 57, 2930−2941

mix solution), which is supplied from Agilent Technologies. Data were processed via Bruker DataAnalysis software (version 4.0). When the calculated and experimental masses were compared, the error was as expected (<2 ppm), confirming ≥95% of purity for all compounds.

(2*E*,2′*E*)-1,1′-(1,4-Phenylene)bis(3-(4-methoxyphenyl)prop-2-en-1-one) (1a). Yield 79%, yellow solid, mp 210−210.5 °C. ^{1}H NMR (200 MHz, $CDCl_3$) δ/ppm 8.10 (s, 4H, H2′, H3′, H5′, H6′), 7.88 (d, 2H, Hβ, Hβ'', J = 15.5 Hz), 7.63 (d, 4H, H2, H2″, H6, H6″, J = 8.8 Hz), 7.41 (d, 2H, Hα, Hα'', J = 15.6 Hz), 6.96 (d, 4H, H3, H3″, H5, H5″, J = 8.8 Hz), 3.87 (s, 6H, p-OCH_3). ^{13}C NMR (50 MHz, $CDCl_3$) δ/ppm 190.1 (C═O), 161.9 (C4, C4″), 145.5 (Cβ, Cβ''), 141.4 (C1′, C4′), 130.7 (C2, C2″, C6, C6″), 128.5 (C2′, C3′, C5′, C6′), 127.4 (C1, C1″), 119.6 (Cα, Cα''), 111.4 (C3, C3″, C5, C5″), 55.4 (p-OCH_3). HRMS (APPI+) m/z calculated for $C_{26}H_{22}O_4$ [M^+], 399.1591; found, 399.1594.

(2*E*,2′*E*)-1,1′-(1,4-Phenylene)bis(3-(3,4,5-trimethoxyphenyl)-prop-2-en-1-one) (1b). Yield 82%, yellow solid, mp 223−224 °C. ^{1}H NMR (400 MHz, $CDCl_3$) δ/ppm 8.12 (s, 4H, H2′, H3′, H5′, H6′), 7.75 (d, 2H, Hβ, Hβ'', J = 15.6 Hz), 7.40 (d, 2H, Hα, Hα'', J = 15.6 Hz), 6.89 (s, 4H, H2, H2″, H6, H6″), 3.94 (s, 12H, m-OCH_3), 3.92 (s, 6H, p-OCH_3). ^{13}C NMR (100 MHz, $CDCl_3$) δ/ppm 190.1 (C═O), 153.5 (C3, C3″, C5, C5″), 146.0 (Cβ, Cβ''), 141.3 (C1′, C4′), 130.0 (C4, C4″), 128.6 (C2′, C3′, C5′, C6′), 121.2 (Cα, Cα''), 105.8 (C2, C2″, C6, C6″), 104.9 (C1, C1″), 61.0 (p-OCH_3), 58.2 (m-OCH_3). HRMS (APPI+) m/z calculated for $C_{30}H_{30}O_8$ [M^+], 519.2013; found, 519.2019.

(2*E*,2′*E*)-1,1′-(1,4-Phenylene)bis(3-(3,4-dimethoxyphenyl)-prop-2-en-1-one) (1c). Yield 84%, yellow solid, mp 176.5−177 °C. ^{1}H NMR (400 MHz, $CDCl_3$) δ/ppm 8.11 (s, 4H, H2′, H3′, H5′, H6′), 7.79 (d, 2H, Hβ, Hβ'', J = 15.6 Hz), 7.39 (d, 2H, Hα, Hα'', J = 15.6 Hz), 7.27 (dd, 2H, H6, H6″, J = 8.2 Hz, J = 1.9 Hz), 7.18 (d, 2H, H2, H2″, J = 1.9 Hz), 6.92 (d, 2H, H5, H5″, J = 8.2 Hz), 3.97 (s, 6H, m-OCH_3), 3.95 (s, 6H, p-OCH_3). ^{13}C NMR (50 MHz, $CDCl_3$) δ/ppm 190.1 (C═O), 151.7 (C3, C3″), 149.3 (C4, C4″), 145.9 (Cβ, Cβ''), 141.4 (C1′, C4′), 128.5 (C2′, C3′, C5′, C6′), 127.6 (C1, C1″), 123.4 (Cα, Cα''), 119.8 (C6, C6″), 111.1 (C2, C2″), 110.2 (C5, C5″), 55.9 (m-OCH_3, p-OCH_3). HRMS (APPI+) m/z calculated for $C_{28}H_{26}O_6$ [M^+], 459.1802; found, 459.1808.

(2*E*,2′*E*)-1,1′-(1,4-Phenylene)bis(3-(benzo[*d*][1,3]dioxol-5-yl)-prop-2-en-1-one) (1d). Yield 76%, yellow solid, mp 268−269 °C. ^{1}H NMR (200 MHz, $CDCl_3$) δ/ppm 8.29 (s, 4H, H2′, H3′, H5′, H6′), 7.85 (m, 4H, Hβ, Hβ'', Hα, Hα''), 7.70 (s, 2H, H2, H2″), 7.37 (d, 2H, H6, H6″, J = 8.0 Hz), 7.02 (d, 2H, H5, H5″, J = 7.9 Hz), 6.13 (s, 4H, CH_2, CH_2''). ^{13}C NMR (50 MHz, $CDCl_3$) δ/ppm 189.1 (C═O), 150.2 (C3, C3″), 148.5 (C4, C4″), 145.3 (Cβ, Cβ''), 141.2 (C1′, C4′), 129.5 (C1, C1″), 129.1 (C2′, C3′, C5′, C6′), 126.7 (Cα, Cα''), 120.4 (C6, C6″), 109.0 (C5, C5″), 107.5 (C2, C2″), 102.1 (CH_2, CH_2''). HRMS (APPI+) m/z calculated for $C_{26}H_{18}O_6$ [M^+], 427.117 61; found, 427.117 58.

(2*E*,2′*E*)-1,1′-(1,4-Phenylene)bis(3-(2,5-dimethoxyphenyl)-prop-2-en-1-one) (1e). Yield 82%, yellow solid, mp 170−170.5 °C. ^{1}H NMR (400 MHz, $CDCl_3$) δ/ppm 8.10 (d, 2H, Hβ, Hβ'', J = 16.0 Hz), 8.10 (s, 4H, H2′, H3′, H5′, H6′), 7.59 (d, 2H, Hα, Hα'', J = 15.6 Hz), 7.18 (d, 2H, H2, H2″, J = 3.0 Hz), 6.97 (dd, 2H, H4, H4″, J = 8.9 Hz, J = 3.0 Hz), 6.89 (d, 2H, H5, H5″, J = 8.9 Hz), 3.88 (s, 6H, o-OCH_3), 3.83 (s, 6H, m-OCH_3). ^{13}C NMR (100 MHz, $CDCl_3$) δ/ppm 190.7 (C═O), 153.4 (C6, C6″), 141.3 (Cβ, Cβ''), 141.1 (C1′, C4′), 128.6 (C2′, C3′, C5′, C6′), 124.1 (Cα, Cα''), 122.9 (C1, C1″), 117.6 (C5, C5″), 113.8 (C4, C4″), 112.4 (C2, C2″), 56.1 (o-OCH_3), 55.8 (m-OCH_3). HRMS (APPI+) m/z calculated for $C_{28}H_{26}O_6$ [M^+], 459.180 22; found, 459.180 16.

(2*E*,2′*E*)-1,1′-(1,4-Phenylene)bis(3-(naphthalen-2-yl)prop-2-en-1-one) (1f). Yield 80%, light yellow solid, mp 248−249 °C. ^{1}H NMR (400 MHz, $CDCl_3$) δ/ppm 8.11 (s, 4H, H2′, H3′, H5′, H6′), 8.00 (d, 2H, Hβ, Hβ'', J = 15.9 Hz), 7.62 (d, 2H, Hα, Hα'', J = 15.7 Hz), 7.90−7.52 (m, 14H, naphthyl ring). ^{13}C NMR (100 MHz, $CDCl_3$) δ/ppm 189.9 (C═O), 145.9 (Cβ, Cβ''), 141.7 (C1′, C4′), 139.8 (C2, C2″), 134.5 (C4, C4″), 133.3 (C4a, C4a″), 132.0 (C8a, C8a″), 130.9 (C8, C8″), 128.8 (C5, C5″), 128.6 (C2′, C3′, C5′, C6′), 127.8 (C7, C7″), 127.5 (C6, C6″), 126.8 (C1, C1″), 123.5 (C3, C3″), 121.9 (Cα, Cα''). HRMS (APPI+) m/z calculated for $C_{32}H_{22}O_2$ [M^+], 439.1693; found, 439.1689.

(2*E*,2′*E*)-1,1′-(1,4-Phenylene)bis(3-(naphthalen-1-yl)prop-2-en-1-one) (1g). Yield 81%, yellow solid, mp 230−231 °C. ^{1}H NMR (200 MHz, $CDCl_3$) δ/ppm 8.72 (d, 2H, Hβ, Hβ'', J = 15.4 Hz), 8.21 (s, 4H, H2′, H3′, H5′, H6′), 7.65 (d, 2H, Hα, Hα'', J = 15.5 Hz), 8.29−7.55 (m, 14H, naphthyl ring). ^{13}C NMR (50, MHz, $CDCl_3$) δ/ppm 189.8 (C═O), 142.6 (Cβ, Cβ''), 141.3 (C1′, C4′), 133.7 (C1, C1″), 132.0 (C4a, C4a″), 131.7 (C8a, C8a″), 128.7 (C2′, C3′, C4′, C6′), 127.0 (C4, C4″), 126.3 (C7, C7″), 125.4 (C3, C3″), 125.2 (C8, C8″), 124.4 (Cα, Cα''), 123.3 (C2, C2″). HRMS (APPI+) m/z calculated for $C_{32}H_{22}O_2$ [M^+], 439.1693; found, 439.1699.

(2*E*,2′*E*)-1,1′-(1,4-Phenylene)bis(3-phenylprop-2-en-1-one) (1h). Yield 92%, light yellow solid, mp 200−201 °C. ^{1}H NMR (200 MHz, $CDCl_3$) δ/ppm 8.12 (s, 4H, H2′, H3′, H5′, H6′), 7.85 (d, 2H, Hβ, Hβ'', J = 15.6 Hz), 7.67 m, 4H, H2, H2″, H6, H6″), 7.53 (d, 2H, Hα, Hα'', J = 15.6 Hz), 7.46 (m, 6H, H3, H3″, H4, H4″, H5, H5″). ^{13}C NMR (50 MHz, $CDCl_3$) δ/ppm 190.0 (C═O), 145.8 (Cβ, Cβ''), 141.3 (C1′, C4′), 134.6 (C1, C1″), 130.8 (C4, C4″), 129.0 (C2, C2″, C6, C6″), 128.6 (C2′, C3′, C5′, C6′), 128.5 (C3, C3″, C5, C5″), 121.9 (Cα, Cα''). HRMS (APPI+) m/z calculated for $C_{24}H_{18}O_2$ [M^+], 339.1380; found, 339.1376.

(2*E*,2′*E*)-1,1′-(1,4-Phenylene)bis(3-(2,4,5-trimethoxyphenyl)-prop-2-en-1-one) (1i). Yield 90%, yellow solid, mp 224.5−225 °C. ^{1}H NMR (200 MHz, $CDCl_3$) δ/ppm 8.09 (s, 4H, H2′, H3′, H5′, H6′), 8.12 (d, 2H, Hβ, Hβ'', J = 15.6 Hz), 7,46 (d, 2H, Hα, Hα'', J = 15.6 Hz), 7.14 (s, 2H, H6, H6″), 6.53 (s, 2H, H3, H3″), 3.96 (s, 6H, p-OCH_3), 3.92 (s, 12H, o-CH_3, m-OCH_3). ^{13}C NMR (100 MHz, $CDCl_3$) δ/ppm 190.8 (C═O), 154.8 (C2, C2″), 152.8 (C4, C4″), 143.2 (C5, C5″), 141.6 (C1, C1″), 141.0 (C1′, C4′), 128.5 (C2′, C3′, C5′, C6′), 120.1 (Cα, Cα''), 111.3 (C6, C6″), 96.6 (C3, C3″), 56.5 (p-OCH_3), 56.0 (o-OCH_3, m-OCH_3). HRMS (APPI+) m/z calculated for $C_{30}H_{30}O_8$ [M^+], 519.2013; found, 519.2011.

(2*E*,2′*E*)-1,1′-(1,4-Phenylene)bis(3-(4-carboxyphenyl)prop-2-en-1-one) (1j). Yield 61%, light yellow solid, mp >350 °C. ^{1}H NMR (200 MHz, DMSO-d_6) δ/ppm 8.33 (s, 2H, COOH), 8.29 (d, 4H, H2, H2″, H6, H6″, J = 8.4 Hz), 8.12 (d, 4H, H3, H3″, H5, H5″, J = 8.5 Hz), 8.05 (m, 2H, Hβ, Hβ''), 8.03 (s, 4H, H2′, H3′, H5′, H6′), 7.84 (d, 2H, Hα, Hα'', J = 15.6 Hz). ^{13}C NMR (100 MHz, DMSO-d_6) δ/ppm 189.4 (C═O), 167.2 (COOH), 143.7 (Cβ, Cβ''), 141.0 (C1′, C4′), 139.0 (C1, C1″), 132.7 (C4, C4″), 130.1 (C2′, C3′, C5′, C6′), 129.4 (C3, C3″, C5, C5″), 128.9 (C2, C2″, C6, C6″), 124.6 (Cα, Cα''). HRMS (APPI+) m/z calculated for $C_{26}H_{18}O_6$ [M^+], 425.1020; found, 425.1023.

(2*E*,2′*E*)-1,1′-(1,4-Phenylene)bis(3-(2,4,6-trimethoxyphenyl)-prop-2-en-1-one) (1k). Yield 83%, yellow solid, mp 278−279 °C. ^{1}H NMR (200 MHz, $CDCl_3$) δ/ppm 8.28 (d, 2H, Hβ, Hβ'', J = 15.9 Hz), 8.07 (s, 4H, H2′, H3′, H5′, H6′), 7.87 (d, 2H, Hα, Hα'', J = 15.8 Hz), 6.15 (s, 4H, H3, H3″, H5, H5″), 3.92 (s, 12H, o-OCH_3), 3.87 (s, 6H, p-OCH_3). ^{13}C NMR (50 MHz, $CDCl_3$) δ/ppm 191.8 (C═O), 161.8 (C2, C2″, C6, C6″), 158.4 (C4, C4″), 142.1 (Cβ, Cβ''), 136.8 (C1′, C4′), 128.4 (C2′, C3′, C5′, C6′), 125.9 (Cα, Cα''), 106.6 (C1, C1″), 90.5 (C3, C3″, C5, C5″), 55.7 (o-OCH_3), 55.2 (o-OCH_3). HRMS (APPI+) m/z calculated for $C_{30}H_{30}O_8$ [M^+], 519.2013; found, 519.2009.

(2*E*,2′*E*)-1,1′-(1,4-Phenylene)bis(3-(4-hydroxy-3-methoxyphenyl)prop-2-en-1-one) (1l). Yield 60%, brown solid, mp 140−141.5 °C. ^{1}H NMR (200 MHz, $CDCl_3$) δ/ppm 8.07 (s, 4H, H2′, H3′, H5′, H6′), 7.77 (d, 2H, Hβ, Hβ'', J = 15.6 Hz), 7.35 (d, 2H, Hα, Hα'', J = 15.6 Hz), 7.24 (dd, 2H, H6, H6″, J = 8.2 Hz, J = 1.9 Hz), 7.15 (d, 2H, H2, H2″, J = 1.8 Hz), 6.97 (d, 2H, H5, H5″, J = 8.2 Hz), 3.98 (s, 6H, m-OCH_3). ^{13}C NMR (50 MHz, $CDCl_3$) δ/ppm 190.1 (C═O), 148.6 (C3, C3″), 146.8 (C4, C4″), 146.2 (Cβ, Cβ''), 142.0 (C1′, C4′), 128.5 (C2′, C3′, C5′, C6′), 127.1 (C1, C1″), 123.6 (Cα, Cα''), 119.5 (C6, C6″), 114.9 (C5, C5″), 110.1 (C2, C2″), 56.0 (m-OCH_3). HRMS (APPI+) m/z calculated for $C_{26}H_{22}O_6$ [M^+], 431.1489; found, 431.1483.

(2*E*,2′*E*)-1,1′-(1,4-Phenylene)bis(3-(quinoxalin-6-yl)prop-2-en-1-one) (1m). Yield 89%, light yellow solid, mp > 350 °C. ^{1}H NMR (200 MHz, $CDCl_3$) δ/ppm 8.90 (m, 4H, H4, H4″, H5, H5″),

8.37 (d, 2H, H2, H2″, J = 1.5 Hz), 8.22 (s, 4H, H2′, H3′, H5′, H6′), 8.14 (m, 4H, H7, H7″, H8, H8″), 8.07 (d, 2H, Hβ, Hβ″, J = 15.7 Hz), 7.76 (d, 2H, Hα, Hα″, J = 15.6 Hz). ^{13}C NMR (50 MHz, $CDCl_3$) δ/ppm 189.2 (C═O), 146.0 (Cβ, Cβ″), 145.6 (C4, C4″), 144.0 (C5, C5″), 143.7 (C3, C3″), 143.0 (C6, C6″), 141.1 (C1′, C4′), 136.3 (C1, C1″), 130.8 (C7, C7″), 130.2 (C2, C2″), 128.9 (C2′, C3′, C5′, C6′), 128.4 (C8, C8″), 124.0 (Cα, Cα″). HRMS (APPI+) m/z calculated for $C_{28}H_{18}N_4O_2$ [M^+], 443.1503; found, 443.1501.

(2*E*,2′*E*)-1,1′-(1,4-Phenylene)bis(3-(4-(dimethylamino)-phenyl)prop-2-en-1-one) (1n). Yield 62%, red solid, mp 204−205 °C. ^{1}H NMR (400 MHz, $CDCl_3$) δ/ppm 8.07 (s, 4H, H2′, H3′, H5′, H6′), 7.81 (d, 2H, Hβ, Hβ″, J = 15.2 Hz), 7.55 (d, 4H, H2, H2″, H6, H6″, J = 8.6 Hz), 7.33 (d, 2H, Hα, Hα″, J = 15.6 Hz), 6.69 (d, 4H, H3, H3″, H5, H5″, J = 8.9 Hz), 3.04 (s, 12H, $N(CH_3)_2$). ^{13}C NMR (100 MHz, $CDCl_3$) δ/ppm 190.1 (C═O), 152.1 (C4, C4″), 146.6 (Cβ, Cβ″), 141.7 (C1′, C4′), 130.6 (C6, C6″), 128.3 (C2′, C3′, C5′, C6′), 122.3 (Cα, Cα″), 116.6 (C1, C1″), 111.8 (C5, C5″), 40.1 ($N(CH_3)_2$). HRMS (APPI+) m/z calculated for $C_{28}H_{28}N_2O_2$ [M^+], 425.2224; found, 425.2218.

(2*E*,2′*E*)-1,1′-(1,4-Phenylene)bis(3-(4-(dimethylamino)-naphthalen-1-yl)prop-2-en-1-one) (1o). Yield 59%, red solid, mp 159−160 °C. ^{1}H NMR (200 MHz, $CDCl_3$) δ/ppm 8.66 (d, 2H, Hβ, Hβ″, J = 15.4 Hz), 8.07 (s, 4H, H2′, H3′, H5′, H6′), 7.52 (d, 2H, Hα, Hα″, J = 15.4 Hz), 8.27−7.05 (m, 12H, naphthyl ring), 2.98 (s, 12H, N-$(CH_3)_2$). ^{13}C NMR (50 MHz, $CDCl_3$) δ/ppm 198.3 (C═O), 154.0 (C4, C4″), 142.8 (Cβ, Cβ″), 139.5 (C1′, C4′), 133.2 (C8a, C8a″), 128.5 (C4a, C4a″), 128.3 (C2′, C3′, C5′, C6′), 126.9 (C1, C1″), 126.0 (C7, C7″), 125.2 (C6, C6″), 125.1 (C5, C5″), 124.9 (C8, C8″), 123.6 (Cα, Cα″), 121.7 (C2, C2″), 113.2 (C3, C3″), 44.8 (N-$(CH_3)_2$). HRMS (APPI+) m/z calculated for $C_{36}H_{32}N_2O_2$ [M^+], 525.2537; found, 525.2534.

(2*E*,2′*E*)-1,1′-(1,4-Phenylene)bis(3-(2,6-dimethoxyphenyl)-prop-2-en-1-one) (1p). Yield 91%, yellow solid, mp 253−254 °C. ^{1}H NMR (200 MHz, $CDCl_3$) δ/ppm 8.30 (d, 2H, Hβ, Hβ″, J = 16.0 Hz), 8.10 (s, 4H, H2′, H3′, H5′, H6′), 8.00 (d, 2H, Hα, Hα″, J = 15.9 Hz), 7.33 (dd, 2H, H4, H4″, J = 8.4 Hz, J = 8.3 Hz), 6.61 (d, 4H, H3, H3″, H5, H5″, J = 8.4 Hz), 3.93 (s, 12H, o-OCH_3). ^{13}C NMR (50 MHz, $CDCl_3$) δ/ppm 191.8 (C═O), 160.4 (C2, C2″, C6, C6″), 141.6 (Cβ, Cβ″), 136.5 (C1′, C4′), 131.8 (C4, C4″), 128.5 (C2′, C3′, C5′, C6′), 124.7 (Cα, Cα″), 112.6 (C1, C1″), 103.7 (C3, C3″, C5, C5″), 55.8 (o-OCH_3). HRMS (APPI+) m/z calculated for $C_{28}H_{26}O_6$ [M^+], 459.1802; found, 459.1808.

(2*E*,2′*E*)-1,1′-(1,4-Phenylene)bis(3-(2,3,4-trimethoxyphenyl)-prop-2-en-1-one) (1q). Yield 93%, yellow solid, mp 178−179 °C. ^{1}H NMR (200 MHz, $CDCl_3$) δ/ppm 8.11 (s, 4H, H2′, H3′, H5′, H6′), 8.03 (d, 2H, Hβ, Hβ″, J = 15.9 Hz), 7.56 (d, 2H, Hα, Hα″, J = 15.7 Hz), 7.42 (d, 2H, H6, H6″, J = 8.8 Hz), 6.74 (d, 2H, H5, H5″, J = 8.8 Hz), 3.97 (s, 6H, o-OCH_3), 3.93 (s, 6H, p-OCH_3), 3.90 (s, 3H, m-OCH_3). ^{13}C NMR (50 MHz, $CDCl_3$) δ/ppm 190.4 (C═O), 156.0 (C4, C4″), 153.9 (C2, C2″), 142.5 (Cβ, Cβ″), 141.5 (C3, C3″), 141.0 (C1′, C4′), 128.5 (C2′, C3′, C5′, C6′), 124.0 (C1, C1″), 121.7 (Cα, Cα″), 121.2 (C6, C6″), 107.6 (C5, C5″), 61.3 (p-OCH_3), 60.8 (m-OCH_3), 56.0 (o-OCH_3). HRMS (APPI+) m/z calculated for $C_{30}H_{30}O_8$ [M^+], 519.2013; found, 519.2019.

(2*E*,2′*E*)-3,3′-(1,4-Phenylene)bis(1-(4-methoxyphenyl)prop-2-en-1-one) (2a). Yield 83%, yellow solid, mp 248−249 °C. ^{1}H NMR (200 MHz, $CDCl_3$) δ/ppm 8.06 (d, 4H, H2′, H2″, H6′, H6″, J = 8.9 Hz), 7.81 (d, 2H, Hβ′, Hβ″, J = 15.6 Hz), 7.69 (s, 4H, H2, H3, H5, H6), 7.59 (d, 2H, Hα′, Hα″, J = 15.6 Hz), 7.00 (d, 4H, H3′, H3″, H5′, H5″, J = 8.9 Hz), 3.91 (s, 6H, p-OCH_3). ^{13}C NMR (50 MHz, $CDCl_3$) δ/ppm 188.4 (C═O), 163.5 (C4′, C4″), 142.7 (Cβ′, Cβ″), 136.9 (C1, C4), 130.8 (C2′, C2″, C6′, C6″), 130.6 (C1″, C1″), 128.8 (C2, C3, C5, C6), 122.8 (Cα′, Cα″), 113.9 (C3′, C3″, C5′, C5″), 55.4 (p-OCH_3). HRMS (APPI+) m/z calculated for $C_{26}H_{22}O_4$ [M^+], 399.1591; found, 399.1596.

(2*E*,2′*E*)-3,3′-(1,4-Phenylene)bis(1-(3,4,5-trimethoxyphenyl)-prop-2-en-1-one) (2b). Yield 80%, yellow solid, mp 190−190.5 °C. ^{1}H NMR (400 MHz, $CDCl_3$) δ/ppm 7.82 (d, 2H, Hβ′, Hβ″, J = 15.6 Hz), 7.71 (s, 4H, H2, H3, H5, H6), 7.54 (d, 2H, Hα′, Hα″, J = 15.6 Hz), 7.29 (s, 4H, H2′, H2″, H6′, H6″), 3.96 (s, 12H, m-OCH_3), 3.95 (s, 6H, p-OCH_3). ^{13}C NMR (100 MHz, $CDCl_3$) δ/ppm 190.5 (C═O), 188.8 (C═O′), 153.1 (C3′, C5′, C3″, C5″), 143.4 (C4′, C4″), 142.8 (Cβ′, Cβ″), 136.8 (C1, C4), 133.2 (C1′, C1″), 128.9 (C2, C3, C5, C6), 122.7 (Cα′, Cα″), 106.1 (C2′, C6′, C2″, C6″), 61.0 (p-OCH_3), 56.4 (m-OCH_3). HRMS (APPI+) m/z calculated for $C_{30}H_{30}O_8$ [M^+], 519.2013; found, 519.2017.

(2*E*,2′*E*)-3,3′-(1,4-Phenylene)bis(1-(3-methoxyphenyl)prop-2-en-1-one) (2c). Yield 87%, yellow solid, mp 176−177 °C. ^{1}H NMR (400 MHz, $CDCl_3$) δ/ppm 7.81 (d, 2H, Hβ′, Hβ″, J = 15.6 Hz), 7.69 (s, 4H, H2, H3, H5, H6), 7.62 (d, 2H, H6′, H6″, J = 7.8 Hz), 7.56 (d, 2H, Hα′, Hα″, J = 15.6 Hz), 7.55 (d, 2H, H2′, H2″, J = 1.5 Hz), 7.43 (dd, 2H, H5′, H5″, J = 8.2 Hz, J = 7.8 Hz), 7.15 (dd, 2H, H4′, H4″, J = 8.2 Hz, J = 2.7 Hz), 3.89 (s, 6H, m-OCH_3). ^{13}C NMR (100 MHz, $CDCl_3$) δ/ppm 189.9 (C═O), 159.9 (C3′, C3″), 143.5 (Cβ′, Cβ″), 139.4 (C1′, C1″), 136.8 (C1, C4), 129.6 (C5′, C5″), 128.9 (C2, C3, C5, C6), 123.0 (Cα′, Cα″), 121.0 (C6′, C6″), 119.4 (C4′, C4″), 112.8 (C2′, C2″), 55.5 (m-OCH_3). HRMS (APPI+) m/z calculated for $C_{26}H_{22}O_4$ [M^+], 399.1591; found, 399.1585.

(2*E*,2′*E*)-3,3′-(1,4-Phenylene)bis(1-(3,4-dimethoxyphenyl)-prop-2-en-1-one) (2d). Yield 91%, yellow solid, mp 198−199 °C. ^{1}H NMR (400 MHz, $CDCl_3$) δ/ppm 7.81 (d, 2H, Hβ′, Hβ″, J = 15.6 Hz), 7.71 (m, 2H, H6′, H6″), 7.70 (s, 4H, H2, H3, H5, H6), 7.64 (m, 2H, H2′, H2″), 7.61 (d, 2H, Hα′, Hα″, J = 15.6 Hz), 6.95 (d, 2H, H5, H5″, J = 8,20 Hz), 3.98 (s, 12H, m-OCH_3, p-OCH_3). ^{13}C NMR (100 MHz, $CDCl_3$) δ/ppm 183.5 (C═O), 149.9 (C4′, C4″), 149.3 (C3′, C3″), 142.7 (Cβ′, Cβ″), 136.8 (C1, C4), 131.5 (C6′, C6″), 130.1 (C1′, C1″), 128.8 (C2, C3, C5, C6), 122.5 (Cα′, Cα″), 110.7 (C5′, C5″), 109.9 (C2′, C2″), 56.0 (m-OCH_3, p-OCH_3). HRMS (APPI+) m/z calculated for $C_{28}H_{26}O_6$ [M^+], 459.1802; found, 459.1804.

(2*E*,2′*E*)-3,3′-(1,4-Phenylene)bis(1-(2,4-dimethoxyphenyl)-prop-2-en-1-one) (2e). Yield 83%, yellow solid, mp 182.5−183 °C. ^{1}H NMR (400 MHz, $CDCl_3$) δ/ppm 7.78 (d, 2H, H3′, H3″, J = 8.5 Hz), 7.68 (d, 2H, Hβ′, Hβ″, J = 15.6 Hz), 7.61 (s, 4H, H2, H3, H5, H6), 7.58 (d, 2H, Hα′, Hα″, J = 15.6 Hz), 6.58 (dd, 2H, H4′, H4″, J = 8.5 Hz, J = 2.3 Hz), 6.51 (d, 2H, H6′, H6″, J = 2.3 Hz), 3.92 (s, 3H, p-OCH_3), 3.92 (s, 3H, o-OCH_3′). ^{13}C NMR (100 MHz, $CDCl_3$) δ/ppm 190.1 (C═O), 164.3 (C2′, C2″), 160.4 (C5′, C5″), 140.8 (Cβ′, Cβ″), 137.0 (C1, C4), 130.1 (C1′, C1″), 128.7 (C2, C3, C5, C6), 127.8 (C4′, C4″), 122.0 (Cα′, Cα″), 105.2 (C3′, C3″), 98.6 (C6′, C6″), 55.7 (o-OCH_3, p-OCH3). HRMS (APPI+) m/z calculated for $C_{28}H_{26}O_6$ [M^+], 459.1802; found, 459.1807.

(2*E*,2′*E*)-3,3′-(1,4-Phenylene)bis(1-(benzo[*d*][1,3]dioxol-5-yl)-prop-2-en-1-one) (2f). Yield 78%, light yellow solid, mp 274−275 °C. ^{1}H NMR (200 MHz, $CDCl_3$) δ/ppm 7.97 (s, 4H, H2, H3, H5, H6), 7.96 (m, 6H, Hβ′, Hβ″, H2′, H2″, H6′, H6″), 7.72 (d, 2H, Hα′, Hα″, J = 15.5 Hz), 7.10 (d, 2H, H5′, H5″, J = 8.2 Hz), 6.17 (s, 4H, CH_2′, CH_2″). ^{13}C NMR (50 MHz, DMSO-d_6) δ/ppm 190.0 (C═O), 152.0 (C4′, C4″), 148.4 (C3′, C3″), 142.9 (Cβ′, Cβ″), 137.1 (C1, C4), 129.7 (C2, C3, C5, C6), 125.6 (Cα′, Cα″), 125.1 (C1′, C1″), 118.8 (C6′, C6″), 108.4 (C5′, C5″), 104.1 (C2′, C2″), 102.5 (CH_2′, CH_2″). HRMS (APPI+) m/z calculated for $C_{26}H_{18}O_6$ [M^+], 427.1176; found, 427.1177.

(2*E*,2′*E*)-3,3′-(1,4-Phenylene)bis(1-(2,5-dimethoxyphenyl)-prop-2-en-1-one) (2g). Yield 84%, yellow solid, mp 160−161 °C. ^{1}H NMR (200 MHz, $CDCl_3$) δ/ppm 7.67 (d, 2H, Hβ′, Hβ″, J = 15.7 Hz), 7.62 (s, 4H, H2, H3, H5, H6), 7.46 (d, 2H, Hα′, Hα″, J = 15.7 Hz), 7.21 (d, 2H, H6′, H6″, J = 3.0 Hz), 7.05 (dd, 2H, H4′, H4″, J = 9.0 Hz, J = 3.0 Hz), 6.95 (d, 2H, H3′, H3″, J = 9.0 Hz), 3.88 (s, 6H, o-OCH_3, m-OCH_3). ^{13}C NMR (50 MHz, $CDCl_3$) δ/ppm 190.5 (C═O), 153.6 (C5′, C5″), 152.6 (C2′, C2″), 141.8 (Cβ′, Cβ″), 136.9 (C1, C4), 129.4 (C1′, C1″), 128.8 (C2, C3, C5, C6), 127.6 (Cα′, Cα″), 119.4 (C4′, C4″), 114.4 (C6′, C6″), 113.3 (C3′, C3″), 56.4 (m-OCH_3), 55.8 (o-OCH_3). HRMS (APPI+) m/z calculated for $C_{28}H_{26}O_6$ [M^+], 459.1802; found, 459.1798.

(2*E*,2′*E*)-1,1′-(1,4-Phenylene)bis(3-(naphthalen-2-yl)prop-2-en-1-one) (2h). Yield 89%, light yellow solid, mp 229−230 °C. ^{1}H NMR (200 MHz, $CDCl_3$) δ/ppm 7.91 (d, 2H, Hβ′, Hβ″, J = 15.5 Hz), 7.77 (s, 4H, H2, H3, H5, H6), 7.76 (d, 2H, Hα′, Hα″, J = 15.5 Hz), 8.56−7.55 (m, 14H, naphthyl ring). ^{13}C NMR (50 MHz, DMSO-d_6) δ/ppm 189.3 (C═O), 148.7 (Cβ′, Cβ″), 144.2 (C2′, C2″), 135.4

dx.doi.org/10.1021/jm401879z | J. Med. Chem. 2014, 57, 2930−2941

(C1, C4), 134.7 (C4a′, C4a″), 132.7 (C8a′, C8a″), 130.8 (C1′, C1″), 130.0 (C8′, C8″), 129.2 (C2, C3, C5, C6), 129.1 (C6′, C6″), 128.9 (C4′, C4″), 128.0 (C5′, C5″), 127.0 (C7′, C7″), 124.5 (C3′, C3″), 122.0 (Cα′, Cα″). HRMS (APPI+) m/z calculated for $C_{32}H_{22}O_2$ [M^+], 439.1693; found, 439.1692.

(2*E*,2′*E*)-3,3′-(1,4-Phenylene)bis(1-(3,5-dimethoxyphenyl)-prop-2-en-1-one) (2i). Yield 92%, yellow solid, mp 178−179 °C. ^{1}H NMR (400 MHz, $CDCl_3$) δ/ppm 7.81 (d, 2H, Hβ′, Hβ″, J = 15.6 Hz), 7.69 (s, 4H, H2, H3, H5, H6), 7.52 (d, 2H, Hα′, Hα″, J = 15.6 Hz), 7.16 (d, 4H, H2′, H6′, H2″, H6″, J = 2.3 Hz), 6.69 (dd, 2H, H4′, H4″, J = 2.3 Hz, J = 2.3 Hz), 3.87 (s, 12H, m-OCH_3). ^{13}C NMR (100 MHz, $CDCl_3$) δ/ppm 189.7 (C═O), 160.9 (C3′, C3″, C5′, C5″), 143.5 (Cβ′, Cβ″), 139.9 (C1′, C1″), 136.8 (C1, C4), 128.9 (C2, C3, C5, C6), 122.9 (Cα′, Cα″), 106.3 (C2′, C2″, C6′, C6″), 105.0 (C4′, C4″), 55.6 (m-OCH_3). HRMS (APPI+) m/z calculated for $C_{28}H_{26}O_6$ [M^+], 459.1802; found, 459.1806.

(2*E*,2′*E*)-3,3′-(1,4-Phenylene)bis(1-(naphthalen-1-yl)prop-2-en-1-one) (2j). Yield 69%, light yellow solid, mp 162−163 °C. ^{1}H NMR (200 MHz, $CDCl_3$) δ/ppm 8.35 (m, 2H, H8′, H8″), 8.00 (d, 2H, H5′, H5″, J = 8.2 Hz), 7.91 (m, 2H, H4′, H4″), 7.78 (d, 2H, H2′, H2″, J = 7.0 Hz), 7.58 β (s, 4H, H2, H3, H5, H6), 7.56 (m, 8H, Hβ′, Hβ″, H3′, H3″, H6′, H6″, H7′, H7″), 7.34 (d, 2H, Hα′, Hα″, J = 16.0 Hz). ^{13}C NMR (50 MHz, $CDCl_3$) δ/ppm 195.1 (C═O), 144.3 (Cβ′, Cβ″), 136.8 (C1, C4), 136.7 (C1′, C1″), 133.8 (C4a′, C4a″), 131.8 (C7′, C7″), 130.4 (C8a′, C8a″), 128.9 (C2, C3, C5, C6), 128.4 (C4′, C4″), 127.9 (C5′, C5″), 127.5 (C2′, C2″), 127.2 (C3′, C3″), 126.5 (C6′, C6″), 125.5 (C8′, C8″), 124.4 (Cα′, Cα″). HRMS (APPI+) m/z calculated for $C_{32}H_{22}O_2$ [M^+], 439.1693; found, 439.1695.

(2*E*,2′*E*)-3,3′-(1,4-Phenylene)bis(1-phenylprop-2-en-1-one) (2k). Yield 90%, light yellow solid, mp 190−190.5 °C. ^{1}H NMR (200 MHz, $CDCl_3$) δ/ppm 8.15 (d, 4H, H2′, H2″, H6′, H6″, J = 7.8 Hz), 8.01 (d, 2H, Hβ′, Hβ″, J = 15.6 Hz), 7.96 (s, 4H, H2, H3, H5, H6), 7.75 (d, 2H, Hα′, Hα″, J = 15.6 Hz), 7.65 (dd, 2H, H4′, H4″, J = 7.0 Hz, J = 7.0 Hz), 7.55 (dd, 4H, H3′, H3″, H5′, H5″, J = 7.8 Hz, J = 7.4 Hz).). ^{13}C NMR (50 MHz, $CDCl_3$) δ/ppm 189.5 (C═O), 143.5 (Cβ′, Cβ″), 137.9 (C1′, C1″), 137.1 (C1, C4), 133.7 (C4′, C4″), 129.8 (C2′, C2″, C6′, C6″), 129.2 (C3′, C3″, C5′, C5″), 129.0 (C2, C3, C5, C6), 123.4 (Cα′, Cα″). HRMS (APPI+) m/z calculated for $C_{24}H_{18}O_2$ [M^+], 339.1380; found, 339.1379.

(2*E*,2′*E*)-3,3′-(1,4-Phenylene)bis(1-(2-methoxyphenyl)prop-2-en-1-one) (2l). Yield 75%, gold yellow solid, mp 146−147 °C. ^{1}H NMR (200 MHz, $CDCl_3$) δ/ppm 7.65 (dd, 2H, H6′, H6″, J = 7.4 Hz, J = 1.5 Hz), 7.63 (d, 2H, Hβ′, Hβ″, J = 16.0 Hz), 7.61 (s, 2H, H2, H3, H5, H6), 7.50 (ddd, 2H, H5′, H5″, J = 7.4 Hz, J = 7.4 Hz, J = 1.5 Hz), 7.43 (d, 2H, Hα′, Hα″, J = 16.0 Hz), 7.05 (dd, 2H, H4′, H4″, J = 7.4 Hz, J = 7.4 Hz), 7.01 (d, 2H, H3′, H3″, J = 8.20 Hz), 3.92 (s, 6H, o-OCH_3). ^{13}C NMR (50 MHz, $CDCl_3$) δ/ppm 182.6 (C═O), 158.1 (C2′, C2″), 141.8 (Cβ′, Cβ″), 136.9 (C1, C4), 133.1 (C4′, C4″), 130.4 (C5′, C5″), 128.8 (C2, C3, C5, C6), 127.8 (C1′, C1″), 120.8 (Cα′, Cα″), 111.6 (C3′, C3″), 55.7 (o-OCH_3). HRMS (APPI+) m/z calculated for $C_{26}H_{22}O_4$ [M^+], 399.1591; found, 399.1593.

(2*E*,2′*E*)-3,3′-(1,4-Phenylene)bis(1-(2,4,5-trimethoxyphenyl)-prop-2-en-1-one) (2m). Yield 81%, yellow solid, mp 222.5−223 °C. ^{1}H NMR (200 MHz, $CDCl_3$) δ/ppm 7.67 (m, 8H, H2, H3, H5, H6, Hβ′, Hβ″), 7.41 (s, 2H, H6′, H6″), 6.55 (s, 2H, H3′, H3″), 3.98 (s, 3H, m-OCH_3), 3.95 (s, 3H, o-OCH_3), 3.91 (s, 3H, p-OCH_3). ^{13}C NMR (50 MHz, $CDCl_3$) δ/ppm 189.5 (C═O), 154.9 (C4′, C4″), 153.8 (C2′, C2″), 143.4 (C5′, C5″), 140.7 (Cβ′, Cβ″), 137.0 (C1, C4), 128.7 (C2, C3, C5, C6), 127.9 (C1′, C1″), 120.3 (Cα′, Cα″), 113.1 (C6′, C6″), 97.0 (C3′, C3″), 56.8 (m-OCH_3), 56.3 (p-OCH_3), 56.1 (o-OCH_3). HRMS (APPI+) m/z calculated for $C_{30}H_{30}O_8$ [M^+], 519.2013; found, 519.2017.

(2*E*,2′*E*)-3,3′-(1,4-Phenylene)bis(1-(4-carboxyphenyl)prop-2-en-1-one) (2n). Yield 69%, yellow solid, mp >350 °C. ^{1}H NMR (200 MHz, $CDCl_3$) δ/ppm 10.07 (s, 2H, COOH), 8.28 (d, 4H, H2′, H2″, H6′, H6″, J = 8.3 Hz), 8.06 (m, 6H, Hβ′, Hβ″, H3′, H3″, H5′, H5″), 8.02 (s, 4H, H2, H3, H5, H6), 7.82 (d, 2H, Hα′, Hα″, J = 15.6 Hz). ^{13}C NMR (50 MHz, $CDCl_3$) δ/ppm 189.4 (C═O), 167.0 (COOH), 144.1 (Cβ′, Cβ″), 141.4 (C1′, C1″), 137.1 (C1, C4), 134.9 (C4′, C4″), 130.0 (C2, C3, C5, C6), 129.2 (C3′, C3″, C5′, C5″), 129.1 (C2′, C2″, C6′, C6″), 123.6 (Cα′, Cα″). HRMS (APPI+) m/z calculated for $C_{26}H_{18}O_6$ [M^+], 425.1020; found, 425.1014.

(2*E*,2′*E*)-3,3′-(1,4-Phenylene)bis(1-(2,4,6-trimethoxyphenyl)-prop-2-en-1-one) (2o). Yield 88%, yellow solid, mp 205−206 °C. ^{1}H NMR (200 MHz, $CDCl_3$) δ/ppm 7.52 (s, 4H, H2, H3, H5, H6), 7.36 (d, 2H, Hβ′, Hβ″, J = 16.0 Hz), 6.98 (d, 2H, Hα′, Hα″, J = 16.0 Hz), 6.16 (s, 4H, H3′, H3″, H5′, H5″), 3.86 (s, 6H, p-OCH_3), 3.77 (s, 12H, o-OCH_3). ^{13}C NMR (50 MHz, $CDCl_3$) δ/ppm 193.8 (C═O), 162.5 (C4′, C4″), 158.9 (C2′, C2″, C6′, C6″), 142.6 (Cβ′, Cβ″), 136.7 (C1, C4), 129.7 (Cα′, Cα″), 128.7 (C2, C3, C5, C6), 111.7 (C1′, C1″), 90.7 (C3′, C3″, C5′, C5″), 55.9 (o-OCH_3), 55.4 (p-OCH_3). HRMS (APPI+) m/z calculated for $C_{30}H_{30}O_8$ [M^+], 519.20134; found, 519.20135.

(2*E*,2′*E*)-3,3′-(1,4-Phenylene)bis(1-(4-hydroxy-3-methoxyphenyl)prop-2-en-1-one) (2p). Yield 62%, yellow solid, mp 220−220.5 °C. ^{1}H NMR (200 MHz, DMSO-d_6) δ/ppm 9.67 (s, 2H, OH), 7.92 (d, 2H, H2′, H2″, J = 2.5 Hz), 7.77 (s, 4H, H2, H3, H5, H6), 7.71 (m, 6H, H6′, H6″, Hα′, Hα″, Hβ′, Hβ″), 6.96 (d, 2H, H5′, H5″, J = 8.2 Hz), 3.95 (s, 3H, m-OCH_3). ^{13}C NMR (50 MHz, DMSO-d_6) δ/ppm 187.1 (C═O), 151. 7 (C3′, C3″), 147.5 (C4′, C4″), 141.6 (Cβ′, Cβ″), 136.3 (C1, C4), 129.6 (C1′, C1″), 128.5 (C2, C3, C5, C6), 123.2 (C6′, C6″), 122.4 (Cα′, Cα″), 114.6 (C5′, C5″), 111.1 (C2′, C2″), 55.5 (m-OCH_3). HRMS (APPI+) m/z calculated for $C_{26}H_{22}O_6$ [M^+], 431.1489; found, 431.1491.

Biology and Biochemistry. Compounds. Mitoxantrone, quercetin, Ko143, ATP, and sodium orthovanadate were purchased from Sigma Aldrich (France). Chromone **1** was obtained as previously described.[24] All other reagents were commercial products of the highest available purity grade.

Cell Cultures. The human fibroblast HEK293 cell line transfected with *ABCG2* (HEK293-*ABCG2*) or the empty vector (HEK293-*pcDNA3.1*), as well as the human lung cancer H460 and H23 cell lines, and pancreas cancer PANC-1 cell line were kindly provided by Drs. R. W. Robey and S. E. Bates (NCI, Bethesda, MD). The HEK293 cell line transfected with *ABCC1* (HEK293-*ABCC1*) or the empty vector (HEK293-*pcDNA5*) was obtained as described,[22] as well as for the NIH-3T3 transfected with *ABCB1* (NIH-3T3-*ABCB1*).[43] The HEK293 cell lines were maintained in Dulbecco's modified Eagle medium (DMEM high glucose), and the cancer cells were maintained in RPMI-1640, supplemented with 10% fetal bovine serum (FBS), 1% penicilin/streptomycin, and in some cases 0.75 mg/mL G418 (for HEK293-*pcDNA3.1* and HEK293-*ABCG2*), 200 μg/mL hygromycin B (for HEK293-*ABCC1* and HEK293-*pcDNA5*), 60 ng/mL colchicine (for NIH-3T3-*ABCB1*), or mitoxantrone at variable concentrations in selected cells: 20 nM in H460, 100 nM in PANC-1, and 10 nM in H23 cell lines.

Inhibition of ABCG2-Mediated Drug Efflux. Cells were seeded at a density of 1.5 × 10^5 cells/well into 24-well culture plates. After a 48 h incubation, the cells were exposed to 5 μM mitoxantrone for 30 min at 37 °C in the presence or absence of compounds at various concentrations, then washed with phosphate buffer saline (PBS) and trypsinized. The intracellular fluorescence was monitored with a FACSCalibur cytometer (Becton Dickinson), using the FL4 channel, and at least 10 000 events were collected. The percentage of inhibition was calculated by using the following equation:

$$\%\ \text{inhibition} = \frac{C - M}{C_{ev} - M} \times 100$$

where C is the intracellular fluorescence of resistant cells (transfected HEK293-*ABCG2* or drug-selected cancer cells) in the presence of compounds and mitoxantrone, M is the intracellular fluorescence of resistant cells in the presence of only mitoxantrone, and C_{ev} is the intracellular fluorescence of control cells (HEK293-pcDNA3.1 or parental cancer cells) in the presence of compounds and mitoxantrone.

Effects on P-Glycoprotein- and MRP1-Mediated Drug Efflux. NIH-3T3 cells transfected with *ABCB1* were seeded at a density of 1.5 × 10^5 cells/well into 24-well culture plates and incubated for 48 h at 37 °C in 5% CO_2, whereas HEK293 cells transfected with *ABCC1* were seeded at 2 × 10^5 cells/well. The cells were respectively exposed to 5 μM mitoxantrone or 0.2 μM calcein-AM for 30 min at 37 °C in

the presence or absence of bis-chalcones at 1 or 10 μM, then washed with phosphate buffer saline (PBS) and trypsinized. The intracellular fluorescence was monitored with a FACSCalibur cytometer (Becton Dickinson), using the FL4 channel to mitoxantrone and FL1 to calcein detection. At least 10 000 events were collected. The percentage of inhibition was calculated relative to NIH-3T3 cells for P-glycoprotein or to HEK293/pcDNA5 cells for MRP1, where the maximal accumulation was equivalent to a complete inhibition.

ATPase Activity Assay. Vanadate-sensitive ATPase activity was measured colorimetrically by determining the liberation of inorganic phosphate from ATP.[44] The Sf9 membranes were prepared as described previously[32] and loaded with cholesterol.[33] The incubation was performed in 96-well plates. Sf9 membranes (0.5 mg/mL) were incubated in a 50 mM Tris-HCl, 50 mM NaCl buffer (pH 8.0) containing the tested compounds with or without sodium orthovanadate (0.33 mM). The reaction was started by the addition of ATP-Mg (3.9 mM), and the plates were incubated for 30 min at 37 °C. The reaction was stopped with sodium dodecyl sulfate (10%) and revealed with a mixture of ammonium molybdate reagent and 10% ascorbic acid (1:4). The absorbance was measured at 880 nm, after a 30 min incubation, using a reader plate.

Mitoxantrone-Induced Cytotoxicity and Chemosensitization by Bis-chalcones. Cell survival was studied using the MTT colorimetric assay.[45] HEK293-*ABCG2* and control HEK293-*pcDNA3.1* cells were seeded at a density of 1×10^4 cells/well into 96-well culture plates and incubated for 24 h at 37 °C in 5% CO_2. Both cell lines were treated with mitoxantrone (at 0−25 nM), and the ABCG2-overexpressing cells were also treated with the bis-chalcones, **1p** at 0.1 μM and **2i** at 0.5 μM, for 72 h. These concentrations, which did not exceed the EC_{50} values of inhibition, were not toxic. Then an amount of 20 μL of the MTT solution (5 mg/mL) was added to each well, and the samples were incubated for 4 h at 37 °C. The culture medium was discarded, and an amount of 100 μL of a DMSO/ethanol (1:1) solution was added to each well and mixed by gentle shaking for 10 min. Absorbance was measured in a microplate reader at 570 nm.

AUTHOR INFORMATION

Corresponding Author

*E-mail: a.dipietro@ibcp.fr. Phone: (+33) 47272 2629. Fax: (+33) 47272 2604.

Notes

The authors declare no competing financial interest.

ACKNOWLEDGMENTS

Drs. R. W. Robey and S. E. Bates, NCI Bethesda, MD, are acknowledged for providing the mitoxantrone-selected cancer cell lines, and Drs. C. Ozvegy-Laczka and B. Sarkadi are acknowledged for the Sf9 membranes overexpressing human ABCG2. E.W. was a recipient of a mobility fellowship from the Brazilian CAPES (Process No. 8792127). P.D.N. and C.G. were recipients of doctoral fellowships from Conselho Nacional de Desenvolvimento Científico e Tecnológico (CNPq), Brazil, and the Ligue Nationale Contre le Cancer, France, respectively. Financial support was provided by the CNRS and Université Lyon 1 (UMR 5086), the Ligue Nationale Contre le Cancer (Equipe Labellisée Ligue 2013), an international grant from French ANR and Hungarian NIH (2010-INT-1101-01) and grants from CNPq, Brazil. We thank Department of Chemistry and Structural Molecular Biology Center from Federal University of Santa Catarina, Brazil, for use of the equipment for chemical characterization of organic compounds, and staff for technical assistance.

ABBREVIATIONS USED

ABC, ATP-binding cassette; BCRP, breast cancer resistance protein (ABCG2); FTC, fumitremorgin C; MRP1, multidrug resistance protein 1 (ABCC1); P-gp, P-glycoprotein (ABCB1)

REFERENCES

(1) Gottesman, M. M. Mechanisms of cancer drug resistance. *Annu. Rev. Med.* **2002**, *53*, 615−627.

(2) Gottesman, M. M.; Ludwig, J.; Xia, D.; Szakács, G. Defeating drug resistance in cancer. *Discovery Med.* **2009**, *6* (31), 18−23.

(3) Szakács, G.; Paterson, J. K.; Ludwig, J. A.; Booth-Genthe, C.; Gottesman, M. M. Targeting multidrug resistance in cancer. *Nat. Rev. Drug Discovery* **2006**, *5* (3), 219−234.

(4) Juliano, R. L.; Ling, V. A surface glycoprotein modulating drug in Chinese hamster ovary cell mutants. *Biochim. Biophys. Acta* **1976**, *455* (1), 152−162.

(5) Cole, S. P.; Bhardwaj, G.; Gerlach, J. H.; Mackie, J. E.; Grant, C. E.; Almquist, K. C.; Stewart, A. J.; Kurz, E. U.; Duncan, A. M. V.; Deeley, R. G. Overexpression of a transporter gene in a multidrug-resistant human lung cancer cell line. *Science* **1993**, *258* (5088), 1650−1654.

(6) Allikmets, R.; Schriml, L. M.; Hutchinson, A.; Romano-Spica, V.; Dean, M. A human placenta-specific ATP-binding cassette gene (ABCP) on chromosome 4q22 that is involved in multidrug resistance. *Cancer Res.* **1998**, *58* (23), 5337−5339.

(7) Doyle, L. A.; Yang, W.; Abruzzo, L. V.; Krogmann, T.; Gao, Y.; Rishi, A. K.; Ross, D. D. A multidrug resistance transporter from human MCF-7 breast cancer cells. *Proc. Natl. Acad. Sci. U.S.A.* **1998**, *95* (26), 15665−15670.

(8) Miyake, K.; Mickley, L.; Litman, T.; Zhan, Z.; Robey, R.; Cristensen, B.; Brangi, M.; Greenberger, L.; Dean, M.; Fojo, T.; Bates, S. E. Molecular cloning of cDNAs which are highly overexpressed in mitoxantrone-resistant cells: demonstration of homology to ABC transport genes. *Cancer Res.* **1999**, *59* (1), 8−13.

(9) Anglicheau, D.; Pallet, N.; Rabant, M.; Marquet, P.; Cassinat, B.; Méria, P.; Beaune, P.; Legendre, C.; Thervet, E. Role of P-glycoprotein in cyclosporine cytotoxicity in the cyclosporine-sirolimus interaction. *Kidney Int.* **2006**, *70* (6), 1019−1025.

(10) Cripe, L. D.; Uno, H.; Paietta, E. M.; Litzow, M. R.; Ketterling, R. P.; Bennett, J. M.; Rowe, J. M.; Lazarus, H. M.; Luger, S.; Tallman, M. S. Zosuquidar, a novel modulator of P-glycoprotein does not improve the outcome of older patients with newly diagnosed acute myeloid leukemia: a randomized, placebo-controlled trial of the Eastern Cooperative Oncology Group 3999. *Blood* **2010**, *116* (20), 4077−4085.

(11) Darby, R. A.; Callaghan, R.; McMahon, R. M. P-glycoprotein inhibition: the past, the present and the future. *Curr. Drug Metab.* **2011**, *12* (8), 722−731.

(12) Vlaming, M. L.; Lagas, J. S.; Schinkel, A. H. Physiological and pharmacological roles of ABCG2 (BCRP): recent findings in Abcg2 knockout mice. *Adv. Drug Delivery Rev.* **2009**, *61* (1), 14−25.

(13) Natarajan, K.; Xie, Y.; Baer, M. R.; Ross, D. D. Role of breast cancer resistance protein (BCRP/ABCG2) in cancer drug resistance. *Biochem. Pharmacol.* **2012**, *83* (8), 1084−1103.

(14) Rabindran, S. K.; He, H.; Singh, M.; Brown, E.; Collins, K. I.; Annable, T.; Greenberger, L. M. Reversal of a novel multidrug resistance mechanism in human colon carcinoma cells by fumitremorgin C. *Cancer Res.* **1998**, *58* (24), 5850−5858.

(15) Allen, J. D.; van Loevezijn, A.; Lakhai, J. M.; van der Valk, M.; van Tellingen, O.; Reid, G.; Schellens, J. H. M.; Koomen, G. J.; Schinkel, A. H. Potent and specific inhibition of the breast cancer resistance protein multidrug transporter in vitro and in mouse intestine by a novel analogue of fumitremorgin C. *Mol. Cancer Ther.* **2002**, *1* (6), 417−425.

(16) Van Loevezijn, A.; Allen, J. D.; Schinkel, A. H.; Koomen, G. J. Inhibition of BCRP-mediated drug efflux by fumitremorgin-type indolyl diketopiperazines. *Bioorg. Med. Chem. Lett.* **2001**, *11* (1), 29−32.

(17) Arnaud, O.; Boumendjel, A.; Gèze, A.; Honorat, M.; Matera, E. L.; Guitton, J.; Stein, W. D.; Bates, S. E.; Falson, P.; Dumontet, C.; Di Pietro, A.; Payen, L. The acridone derivative MBLI-87 sensitizes breast cancer resistance protein-expressing xenografts to irinotecan. *Eur. J. Cancer* **2011**, *47* (4), 640−648.
(18) Ahmed-Belkacem, A.; Pozza, A.; Munoz-Martinez, F.; Bates, S. E.; Castanys, S.; Gamarro, F.; Di Pietro, A.; Pérez-Victoria, J. M. Flavonoid structure−activity studies identify 6-prenylchrysin and tectochrysin as potent and specific inhibitors of breast cancer resistance protein ABCG2. *Cancer Res.* **2005**, *65* (11), 4852−4860.
(19) Yuan, J.; Wong, I. L. K.; Jiang, T.; Wang, S. W.; Liu, T.; Wen, B. J.; Chow, L. M. C.; Sheng, B. W. Synthesis of methylated quercetin derivatives and their reversal activities on Pgp- and BCRP-mediated multidrug resistance tumour cells. *Eur. J. Med. Chem.* **2012**, *54*, 413−422.
(20) Juvale, K.; Pape, V. F.; Wiese, M. Investigation of chalcones and benzochalcones as inhibitors of breast cancer resistance protein. *Bioorg. Med. Chem.* **2012**, *20* (1), 346−355.
(21) Gauthier, C.; Valdameri, G.; Terreux, R.; Kachadourian, R.; Day, B. J.; Winnischofer, S. M.; Rocha, M. E.; Frachet, V.; Ronot, X.; Di Pietro, A.; Boumendjel, A. Investigation of chalcones as selective inhibitors of the breast cancer resistance protein ABCG2: critical role of methoxy substituents in both inhibition and cytotoxicity. *J. Med. Chem.* **2012**, *55* (7), 3193−3200.
(22) Rangel, L. P.; Winter, E.; Gauthier, C.; Terreux, R.; Chiaradia-Delatorre, L. D.; Mascarello, A.; Nunes, R. J.; Yunes, R. A.; Creczynski-Pasa, T. B.; Macalou, S.; Lorendeau, D.; Baubichon-Cortay, H.; Ferreira-Pereira, A.; Di Pietro, A. New structure−activity relationships of chalcone inhibitors of breast cancer resistance protein: poly-specificity toward inhibition and critical substitutions against cytotoxicity. *Drug Des. Dev. Ther.* **2013**, *7*, 1043−1052.
(23) Valdameri, G.; Genoux-Bastide, E.; Peres, B.; Gauthier, C.; Guitton, J.; Terreux, R.; Winnischofer, S. M.; Rocha, M. E.; Boumendjel, A.; Di Pietro, A. Substituted chromones as highly potent nontoxic inhibitors, specific for the breast cancer resistance protein. *J. Med. Chem.* **2012**, *55* (2), 966−970.
(24) Winter, E.; Lecerf-Schmidt, F.; Jabor Gozzi, G.; Peres, B.; Lightbody, M.; Gauthier, C.; Ozvegy-Laczka, C.; Szakacs, G.; Sarkadi, B.; Creczynski-Pasa, T.; Boumendjel, A.; Di Pietro, A. Structure−activity relationships of chromone derivatives toward mechanism of interaction with, and inhibition of, breast cancer resistance protein ABCG2. *J. Med. Chem.* **2013**, *56*, 9849−9860.
(25) Chiaradia, L. D.; Martins, P. G. A.; Cordeiro, M. N. S.; Guido, R. V. C.; Ecco, G.; Andricopulo, A. D.; Yunes, R. A.; Vernal, J.; Nunes, R. J.; Terenzi, H. Synthesis, biological evaluation and molecular modeling of chalcone derivatives as potent inhibitors of *Mycobacterium tuberculosis* protein tyrosine phosphatases (PtpA and PtpB). *J. Med. Chem.* **2012**, *55* (1), 390−402.
(26) Högberg, T.; Bengtsson, S.; Paulis, T. de.; Johansson, L.; Ström, P.; Hall, H.; Ögren, S. O. Potential antipsychotic agents. 5. Synthesis and antidopaminergic properties of substituted 5,6- dimethoxysalicylamides and related compounds. *J. Med. Chem.* **1990**, *33* (4), 1155−1163.
(27) Chiaradia, L. D.; dos Santos, R.; Vitor, C. E.; Vieira, A. A.; Leal, P. C.; Nunes, R. J.; Calixto, J. B.; Yunes, R. A. Synthesis and pharmacological activity of chalcones derived from 2,4,6-trimethoxyacetophenone in RAW 264.7 cells stimulated by LPS: quantitative structure−activity relationships. *Bioorg. Med. Chem.* **2008**, *16* (2), 658−667.
(28) (a) El-Rayyes, N. R.; Al-Johary, A. J. Heterocycles. Part 6. Synthesis of new substituted isoxazoles and pyrazoles. *J. Iraqi Chem. Soc.* **1984**, *9*, 63−72. (b) Harrison, W. T. A.; Ravindra, H. J.; Suresh, K. M. R.; Dharmaprakash, S. M. (2*E*,2*E*′)-3,3′-(1,4-Phenylene)bis[1-(3,4-dimethoxyphenyl)prop-2-en-1-one]. *Acta Crystallogr., Sect. E: Struct. Rep. Online* **2007**, *63*, o3069. (c) Reddy, D.; Bhaskar, S. B.; Eswaraiah, S.; Seshamma, T.; Reddy, M. V. R. Synthesis and antimicrobial activity of some new bis(2-pyrazolino-3-yl)benzenes. *J. Indian Chem. Soc.* **1989**, *66*, 893−896. (d) Zhou, J.; Zhou, J.; Zou, Z.; Feng, J. A facile synthesis of 1,4-bis-(3-aryl-3-oxo-1-propenyl)benzenes under microwave irradiation. *Synth. Commun.* **2002**, *32*, 3389−3392. (e) Yoshitake, O.; Miyazaki, H.; Suzaki, D.; Yamada, Y. Organic electroluminescent device showing luminous efficiency and driving stability. PCT Int. Appl. WO 2005030901 A120050407, 2005. (f) Tsukerman, S. V.; Maslennikova, V. P.; Nikitchenko, V. M.; Lavrushin, V. F. Electron spectra of isomeric *p*-dichalcones and some of their analogs. *Zh. Prikl. Spektrosk.* **1970**, *12*, 91−96. (g) Chitra, M.; Rajendran, T. V.; Duraipandiyan, V.; Rajan, Y. C.; Reuben, J. D. A study on the synthesis and bactericidal activity of certain copolyesters containing bischalcone moiety in the main chain. *Indian J. Sci. Technol.* **2010**, *3*, 890−893. (h) Mobinikhaledi, A.; Kalhor, M.; Jamalifar, H. Synthesis, characterization and antimicrobial activities of some novel bis-chalcones. *Med. Chem. Res.* **2012**, *21*, 1811−1816.
(29) Robey, R. W.; Honjo, Y.; Van de Laar, A.; Miyake, K.; Regis, J. T.; Litman, T.; Bates, S. E. A functional assay for detection of the mitoxantrone resistance protein, MXR (ABCG2). *Biochim. Biophys. Acta* **2001**, *1512* (2), 171−182.
(30) Bessho, Y.; Oguri, T.; Achiwa, H.; Muramatsu, H.; Maeda, H.; Niimi, T.; Sato, S.; Ueda, R. Role of ABCG2 as a biomarker for predicting resistance to CPT-11/SN-38 in lung cancer. *Cancer Sci.* **2006**, *97* (3), 192−198.
(31) Zhou, J.; Wang, C. Y.; Liu, T.; Wu, B.; Zhou, F.; Xiong, J. X.; Wu, H. S.; Tao, J.; Zhao, G.; Yang, M.; Gou, S. M. *World J. Gastroenterol.* **2008**, *14* (6), 925−930.
(32) Ozvegy-Laczka, C.; Varady, G.; Koblos, G.; Ujhelly, O.; Cervenak, J.; Schuetz, J. D. Function-dependent conformational changes of the ABCG2 multidrug transporter modify its interaction with a monoclonal antibody on the cell surface. *J. Biol. Chem.* **2005**, *280* (6), 4219−4227.
(33) Telbisz, A.; Muller, M.; Ozvegy-Laczka, C.; Homolya, L.; Szente, L.; Varadi, A.; Sarkadi, B. Membrane cholesterol selectively modulates the activity of the human ABCG2 multidrug transporter. *Biochim. Biophys. Acta* **2007**, *1768* (11), 2698−2713.
(34) Wollmann, J.; Molnar, J.; Hilgeroth, A. Physicochemical characteristics of novel P-glycoprotein inhibitors of the cage dimeric 1,4-dihydropyridine type. *Med. Chem.* **2006**, *2* (6), 565−568.
(35) Namanja, H. A.; Emmert, D.; Davis, D. A.; Campos, C.; Miller, D. S.; Hrycyna, C. A.; Chmielewski, J. Toward eradicating HIV reservoirs in the brain: inhibiting P-glycoprotein at the blood−brain barrier with prodrug abacavir dimers. *J. Am. Chem. Soc.* **2012**, *134* (6), 2976−2980.
(36) Chan, K. F.; Zhao, Y.; Burkett, B. A.; Wong, I. L.; Chow, L. M.; Chan, T. H. Flavonoid dimers as bivalent modulators for P-glycoprotein-based multidrug resistance: synthetic apigenin homodimers linked with defined-length poly(ethylene glycol) spacers increase drug retention and enhance chemosensitivity in resistant cancer cells. *J. Med. Chem.* **2006**, *49* (23), 6742−6759.
(37) Wong, I. L.; Chan, K. F.; Tsang, K. H.; Lam, C. Y.; Zhao, Y.; Chan, T. H.; Chow, L. M. Modulation of multidrug resistance protein 1 (MRP1/ABCC1)-mediated multidrug resistance by bivalent apigenin homodimers and their derivatives. *J. Med. Chem.* **2009**, *52* (17), 5311−5322.
(38) Chan, K. F.; Wong, I. L.; Kan, J. W.; Yan, C. S.; Chow, L. M.; Chan, T. H. Amine linked flavonoid dimers as modulators of P-glycoprotein-based multidrug resistance: structure−activity relationship and mechanism of modulation. *J. Med. Chem.* **2012**, *55* (5), 1999−2014.
(39) Valdameri, G.; Pereira Rangel, L.; Spatafora, C.; Guitton, J.; Gauthier, C.; Arnaud, O.; Ferreira-Pereira, A.; Falson, P.; Winnischofer, S. M.; Rocha, M. E.; Tringali, C.; Di Pietro, A. Methoxy stilbenes as potent, specific, untransported, and nontoxic inhibitors of breast cancer resistance protein. *ACS Chem. Biol.* **2012**, *7* (2), 322−330.
(40) Boger, D. L.; Soenen, D. R.; Boyce, C. W.; Hedrick, M. P.; Jin, Q. Total synthesis of ningalin B utilizing a heterocyclic azadiene Diels−Ader reaction and discovery of a new class of potent multidrug resistant (MDR) reversal agents. *J. Org. Chem.* **2000**, *65* (8), 2479−2483.

(41) Soenen, D. R.; Hwang, I. H.; Hedrick, M. P.; Boger, D. L. Multidrug resistance reversal activity of key ningalin analogues. *Bioorg. Med. Chem. Lett.* **2003**, *13* (10), 1777−1781.
(42) Zhang, P. Y.; Wong, I. L. K.; Yan, C. S. W.; Zhang, X. Y.; Jiang, T.; Chow, L. M. C.; Wan, S. B. Design and syntheses of permethyl ningalin B analogues: potent multidrug resistance (MDR) reversal agents of cancer cells. *J. Med. Chem.* **2010**, *53* (14), 5108−5120.
(43) Barile, E.; Borriello, M.; Di Pietro, A.; Doreau, A.; Fattorusso, C.; Fattorusso, E.; Lanzotti, V. Discovery of a new series of jatrophane and lathyrane diterpenes as potent and specific P-glycoprotein modulators. *Org. Biomol. Chem.* **2008**, *6* (10), 1756−1762.
(44) Ozvegy, C.; Litman, T.; Szakacs, G.; Nagy, Z.; Bates, S. E.; Varadi, A.; Sarkadi, B. Functional characterization of the human multidrug transporter, ABCG2, expressed in insect cells. *Biochem. Biophys. Res. Commun.* **2001**, *285* (1), 111−117.
(45) Mosmann, T. Rapid colorimetric assay for cellular growth and survival. Application to proliferation and cyto-toxicity assays. *J. Immunol. Methods* **1983**, *65* (1−2), 55−63.